



Article

Doi 10.5943/ppq/16/1/1

Fungi associated with stem canker and gall diseases of mangrove (*Rhizophora mangle*) forest in the North-Eastern Colombian Urabá Gulf

Rodríguez-Zambrano HL¹, Arango-Isaza R², Pardo-Cardona VM², López-Hernández F³, Urrego-Giraldo LE⁴ and Afanador-Kafuri L^{4*}

¹Laboratorio Nacional de Diagnóstico, Instituto Colombiano Agropecuario-ICA, Pasto, Nariño, Colombia

²Escuela de Biociencias, Facultad de Ciencias, Universidad Nacional de Colombia-Medellín, Antioquia, Colombia

³Corporación Colombiana de Investigación Agropecuaria AGROSAVIA, C.I. La Selva, Rionegro, Antioquia, Colombia

⁴Departamento de Ciencias Forestales, Facultad de Ciencias Agrarias, Universidad Nacional de Colombia-Medellín, Antioquia, Colombia

⁵Departamento de Ciencias Agronómicas, Facultad de Ciencias Agrarias, Universidad Nacional de Colombia- Medellín, Antioquia, Colombia

Rodríguez-Zambrano H.L, Arango-Isaza R, Pardo-Cardona V.M, López-Hernández F, Urrego-Giraldo L.E, Afanador-Kafuri L 2026 – Fungi associated with stem canker and gall diseases of mangrove (*Rhizophora mangle*) forest in the North-Eastern Colombian Urabá Gulf. Plant Pathology & Quarantine 16(1), 1–34, Doi 10.5943/ppq/16/1/1

Abstract

This study aimed to identify the fungal species associated with stem canker and gall diseases that affect red mangrove trees in the Urabá Gulf on the northwestern Caribbean coast of Colombia, using morphological, molecular, and pathogenicity approaches. Fungi were obtained from stem and root samples collected in red mangrove individuals recorded in 13 circular plots distributed along the Urabá Gulf mangrove forests. Morphological characteristics and phylogenetic analysis (ITS, TUB2, ACT, EF1- α) were used to identify fungi. The results indicated that the species *Clonostachys* sp., *Cytospora rhizophorae*, *Fusarium* sp., *Lasiodiplodia jatrophiicola*, *Lasiodiplodia theobromae*, *Rugonectria rugulosa*, *Xenoacremonium* sp., and a new genus and/or species within Cryphonectriaceae are the main fungi associated with canker and gall symptoms. This is the first report of these fungi on *Rhizophora mangle* in the mangrove forests of Colombia and contributes to expanding knowledge about *R. mangle* microbiota. Results facilitate the development of future epidemiological and ecological research on red mangroves, providing relevant information for future studies on interactions with these fungi as endophytes and/or pathogens.

Keywords – Biodiversity – Cryphonectriaceae – endophytes – *Lasiodiplodia* – pathogenicity – *Rugonectria*.

Introduction

Mangrove forests are one of the most biologically productive ecosystems that provide countless ecological and economic goods and services for human and animal communities (Duke et al. 2007). The stability of the forest communities is related to the fluvio-marine dynamics that involve river flooding levels, tide amplitude, and coastal geomorphology, which determine local sediment

transport, soil nutrient, and salinity levels (Krauss et al. 2008). However, several factors may contribute to mangrove area reductions, such as coastal erosion, hurricanes, and droughts associated with seasonal climate changes and extreme events (Gilman et al. 2008). Mangroves have developed several adaptations to cope with these environmental changes (Mckee et al. 2007, Krauss et al. 2014, Suárez et al. 2015), persisting in some areas and disappearing in others. Nevertheless, the most significant losses of mangrove forests globally are linked to anthropogenic disturbances, particularly those stemming from deforestation associated with the conversion of mangrove areas to agricultural lands, livestock pastures, as well as the development of the tourism industry and urban infrastructure (Duke et al. 2007). The impact of these human activities on residual mangrove ecosystems is manifested in alterations to soil nutrient availability and water flux dynamics, subsequently leading to species turnover. These environmental transformations can render mangrove trees susceptible to opportunistic pests and pathogens, which may contribute to tree diseases, decline, and mortality.

An assessment of mangroves located in the Urabá Gulf (Urrego et al. 2010) found three mangrove forest types (fringe, basin, and riverine mangroves) (Lugo & Snedaker 1974) that covered around 4,900 ha, mainly determined by coastal geomorphology and fluvio-marine dynamics, and a fourth type in an early successional stage (Urrego et al. 2010). All mangroves showed signs of anthropogenic disturbance, especially related to changes in sediment dynamics associated with the Turbo River diversion in 1954 (Correa & Venette 2004), which have caused species turnover and changes in species dominance and recruitment patterns (Hoyos et al. 2012). In addition, strong shifts in chemical conditions of the soils and flooding waters were also recorded and related to contamination with the residual waters from towns and villages that are thrown into the rivers, streams and finally into the Urabá Gulf (Blanco et al. 2013, Urrego et al. 2014). These water currents also transport chemical substances from upstream mining.

In fringe mangroves, especially those distributed along the Atrato River delta dominated by the red mangrove (*Rhizophora mangle*) (Urrego et al. 2010), most trees showed gall and canker symptoms in woody tissues (stem, branches, and prop roots). Sánchez-Alfárez et al. (2009) also reported attacks by the *Neoteredo reynei* mollusc, weakening the trees of this species. Several research studies worldwide indicate that infections caused by the fungal species *Cytospora rhizophorae* and *Cylindrocarpon didymum* are potential causes of mortality and decline in the structure of the *Rhizophora* tree species exhibiting gall and canker symptoms. (Bernard & Freeman 1982, Wier & Tattar 2000). Research conducted in Thailand during 2018 identified three new species of *Cytospora* associated with mangrove species: *C. lumnitzericola*, *C. thailandica*, and *C. xylocarpi* (Norphanphoun et al. 2018). *Neoscytalidium dimidiatum* was first reported to cause canker and dieback on *Avicennia marina* and *Rhizophora mucronate* in Iran (Goudarzi & Maslehi 2020). Some beetle species have been recorded associated with wood-boring and stem cankers of mangroves in India and may have contributed to the spread of fungal pathogens (Badullage et al. 2023).

The only report of mangrove diseases in Colombia attributes *Agrobacterium tumefaciens* as the likely cause of gall symptoms on the stem and roots of *R. mangle* trees in the Urabá Gulf (Sánchez et al. 2009). However, the causal agent has not been identified (Urrego et al. 2010). The changes in the mangrove forests in Urabá Gulf need the implementation of management strategies and the identification of causal agents for their survival and conservation. This study aimed to identify the fungal species contributing to the development of gall and canker diseases in the mangrove forest of Urabá Gulf in Colombia. Information collected from this study will allow for defining disease management strategies that may contribute to the conservation of mangrove ecosystems.

Materials & Methods

Sampling and Conservation of Fungi

The study was carried out in the fringe mangrove forests of the Urabá Gulf in northern Colombia, located between latitudes 08°33'14, 61" and 07°59'23,45"N and longitudes 76°56'44,91" W and 76°48'40,59" W in Bocas del Atrato township (Fig. 1). The research was focused on fringe

mangrove forests dominated by *Rhizophora mangle* (80%), although *Laguncularia racemosa* and some species from adjacent alluvial rainforest were also present (Urrego et al. 2014).

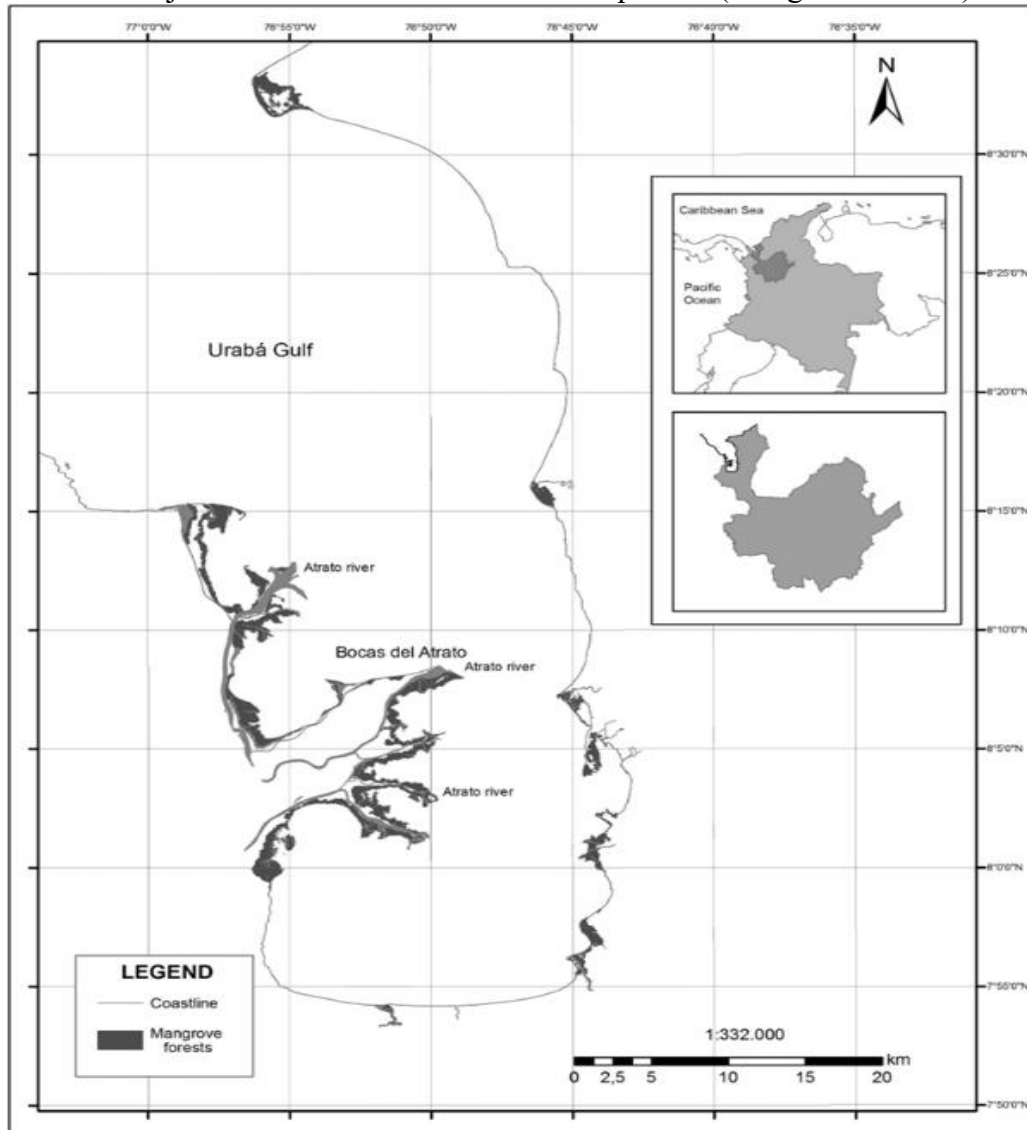


Fig. 1 – Maps showing the locations of sampling sites. The left side of the picture shows the contour of the Urabá Gulf, with the study areas depicted in black. The upper right panel shows the Department of Antioquia highlighted on the Colombian map. The lower right panel highlights the Department of Antioquia and the Urabá Gulf.

A directed sampling was conducted on red mangrove trees found in 13 circular 500 m² plots distributed randomly along the Atrato River delta (Urrego et al. 2014). At each plot, samples were categorized and collected according to symptom type (galls and cankers on stem and roots), sign type (conidia cirrus), and tree class size: adult, trees with diameter (DAP) >10 cm, saplings (DAP <10 cm) and seedlings (height <1 m). To isolate the fungi, 0.5 cm fragments were cut from healthy and diseased tissues. Five fragments of disinfected tissues were then placed on potato dextrose agar (PDA; Difco Laboratories) medium amended with 1 mL of 25% lactic acid per liter (Merck & Co., Inc.) and malt extract agar (MEA: Merck & Co., Inc.). Direct conidia isolation was made from conidial cirrus. Cultures were incubated at room temperature (+/- 24°C) under 8 h light/16 h dark. The evaluation was done at 2-day intervals until fungal colonies began to develop. Portions of mycelium obtained from colony edges were transferred to fresh, acidified potato dextrose agar (APDA) and MEA medium for single spore or hyphal tip isolates. Cultures were stored at 4°C on filter paper and at room temperature (+/- 24°C) on agar blocks in sterile distilled water.

Morphological Identification

A total of 125 fungal isolates were obtained from 80 plant samples. The isolates were preliminarily classified into 24 morphotypes (Mph) or groups, the selection was made based on their origin (affected tissue) and their cultural characteristics in APDA and MEA culture medium. Seven of them were the most predominant per study area and analyzed tissue. Therefore, their morphology and growth rate were analyzed in greater detail. From each group, representative isolates were selected according to their origin (affected tissue) and their cultural characteristics in APDA and MEA culture medium for a total of 42 isolates: Mph 1 (10 isolates), Mph 2 (9 isolates), Mph 3 (12 isolates), Mph 6 (2 isolates), Mph 21 (4 isolates), Mph 14 and 22 (5 isolates).

The representative 42 isolates were examined for their cultural and morphological traits on APDA and MEA medium, incubated at room temperature (+/- 24°C) with light- and dark- cycles of 8 and 16 h, respectively. Colony characteristics (i.e., texture, presence or absence of fruiting bodies, presence or absence of sectors, and mycelial color on the upper and lower surfaces) were determined visually after five weeks. Colony color was rated according to Munsell Soil Color Charts (1990). The size and shape of conidia, conidiophore, and conidioma were observed under a Nikon Eclipse E200 LED compound microscope, photographed with a Nikon digital camera, and measured with a Digital Sight DS-L3 camera controller. For each isolate, 60 conidia and at least two pycnidia from each replicate were analyzed. Identification of fungi at the genus level was done using the taxonomic key of Barnett & Hunter (2006).

DNA Extraction and Amplification

Each isolate was cultured for ten days in an Erlenmeyer flask containing 60 mL of liquid potato dextrose medium plus 60 µL of ampicillin (20 mg/liter) and incubated at room temperature (+/- 24 °C) under 8 h artificial light and 16 h darkness with agitation (150 rpm).

DNA extraction and purification were performed according to the CTAB method modified by Weising et al. (1994). Quality was determined by electrophoresis on a 0.8% agarose gel and quantified by spectrophotometry using a NanoDrop1000 (Thermo Scientific). The DNA was diluted to 50 ng µL⁻¹ as a working solution for polymerase chain reaction (PCR) amplification.

Nucleotide sequences were determined for four PCR nuclear amplicons, including the ribosomal internal transcribed spacer (ITS) region, part of the β-tubulin (TUB2), actin (ACT) and elongation factor 1-alpha (EF1-α) genes. Amplification and sequencing were done using the primer pairs ITS1/ ITS4 (White et al. 1990), Bt2a/Bt2b (Glass & Donaldson 1995), ACT512F/ACT783R (Carbone et al. 1999), and EF1986R/ EF1728F (Carbone & Kohn 1999), respectively.

The PCR amplifications were performed in a 30 µl reaction volume, consisting of 50 µM each primer, 5 U Taq DNA polymerase (Fermentas®, Lithuania), 2.5 mM dNTPs, 1 X Taq buffer, 25 mM MgCl₂, 50 ng DNA template and sterile distilled water. The reactions were performed in a T3 thermal cycler (Biometra®), with an initial denaturation step of 94°C for 3 min; 35 cycles at 94°C for 1 min and 1 min at 55°C (for ITS), 58°C (for TUB2), 56.9°C (for EF1-α) and 61°C (for ACT), plus extension for 2 min at 72°C; and a final extension for 5 min at 72°C. Amplification products were separated by electrophoresis in a 1% agarose gel in 0.5x Tris-borate EDTA buffer, stained with EZ-vision™ DNA dye (Amresco) at 5V cm⁻¹ for 1 h, and visualized using UV light. The DNA of *Colletotrichum brassicicola* was used as positive control for amplification (Afanador et al. 2014). The negative control was high-performance liquid chromatography (HPLC) grade ultrapure water. For each dataset, the ITS, TUB2, ACT, and EF1-α regions were sequenced in both directions using an ABI 3730 DNA sequencing machine as a service provided by Macrogen DNA Services Company® (Seoul, Korea).

Phylogenetic Analysis

Sequences were edited and assembled using Geneious® Bioinformatics software (version 9.1.8: Drummond et al. 2012). Consensus sequences were compared to the NCBI GenBank database using BLAST to determine whether any related sequences were found and those corresponding to

the target genes of the identified taxa were included in the phylogenetic analysis (Supplementary Table S1).

Each dataset was aligned individually using MUSCLE (Edgar 2004) and alignments were adjusted manually as needed. Additionally, each dataset was analyzed using Find Best DNA Models (ML) in MEGA software (Kumar et al. 2018) to find the best model based on BIC scores /Bayesian Information Criterion), AICc value (Akaike Information Criterion corrected), and Maximum Likelihood Value (lnL) to integrate into each phylogeny. Thus, the Kimura 2-parameter (K2P) was the optimal overall model for datasets related to five genera including *Cytospora*, *Rugonectria*, *Clonostachys*, *Lasiodiplodia* and *Xenoacremonium* (Kimura 1980), and Hasegawa-Kishino-Yano (HKY) was the optimal model for Cryphonectriaceae (Mph 1) (Hasegawa et al. 1985).

Maximum likelihood (ML) analyses were performed in MEGA (Kumar et al. 2018) for each dataset to genera *Cytospora*, *Rugonectria*, *Clonostachys*, *Lasiodiplodia*, and *Xenoacremonium*. The ML method used across all five genera was carried out by the Nearest-Neighbor-Interchange (NNI) algorithm with a moderate branch swap filter and partial deletion as Gaps/Missing data treatment. The resampling method for the ML analysis was bootstrap with 10,000 iterations and 10,000 threads. For the specific case of Mph 1, a nuclear multilocus phylogeny was constructed by Bayesian Inference (BI) and ML analyses using TUB2 and ITS markers. Bayesian analyses (BI) were performed with MrBayes v3.1.2 (Ronquist & Huelsenbeck 2003) using Geneious (version 9.1.8: Drummond et al. 2012) for four million generations with four heated chains (temperature = 0.2), one cold chain, burn-in of 10%, and Gamma rate variation. On the other hand, Neighbor-joining reconstruction was performed to cover the main phylogenetic approaches and to demonstrate the consistency regarding the location of the Mph 1 group in phylogenetic trees.

Pathogenicity Tests

Pathogenicity tests were performed under greenhouse and field conditions. The aggressiveness of six representative isolates was evaluated under field conditions by artificially inoculating seven replicates of mangrove saplings and seedlings per isolate using the agar dish and a spore suspension injection method (Afanador et al. 2014) (Table 1). Isolates were selected based on the frequency of morphotypes found in field sampling. Three replicates were used in each of the seven field plots. Each stem was inoculated with a 0.6 cm dish of APDA medium carrying fungal mycelium and then sealed with a Parafilm M strip (Bemis Flexible Packing Company) and an injection of 0.5 mL conidia aqueous suspension adjusted to 1×10^6 conidia mL⁻¹. Seven trees were inoculated with fungus-free APDA, and sterilized distilled water was used as a control. The inoculated area on each tree was then covered with a transparent plastic bag to prevent drying and to protect it from animal damage. The width and length of each resulting lesion were measured in weeks 11 and 30 after inoculation. The lesion area was estimated by assuming a rectangular shape. The greenhouse inoculation was performed on three replicate mangrove seedlings (5.5 months) per isolate using the above-described methods, including inoculation through lenticels. Isolates were inoculated individually and in combination with others. Inoculated plants were then incubated in a humidity chamber (70%) at greenhouse temperature (+/-28 °C) and in complete darkness for five days (Table 1).

Table 1 Inoculation treatments used under field and greenhouse conditions.

Field conditions		
Treatments	Detail	Inoculation method
T1	Control	Agar disc
T2	Control	Sterilized distilled water
T3	Mph 1	Conidial suspension
T4	Mph 1	Agar disc with mycelium
T5	<i>Xenoacremonium</i> sp.	Agar disc with mycelium
T6	<i>Clonostachys</i> sp.	Agar disc with mycelium
T7	Mph 17	Agar disc with mycelium
T8	<i>Rugonectria rugulosa</i>	Agar disc with mycelium

Table 1Continued

Greenhouse conditions	
Treatments	Strain combinations (Day one/a week later)
T1	Control / control
T2	Control only
T3	Mph 1 / Mph 1
T4	<i>Xenoacremonium</i> sp. / Mph 1
T5	<i>Lasiodiplodia jatrophiicola</i> / Mph 1
T6	<i>Clonostachys</i> / Mph 1
T7	Mph 17 / Mph 1
T8	<i>Rugonectria rugulosa</i> / Mph 1
T9	Mph 1 only
T10	<i>L. jatrophiicola</i> only
T11	<i>Rugonectria rugulosa</i> only

The width and length of each resulting lesion were measured from day 5 to 30 after inoculation and then each week to week 25 (176 days) after inoculation. In plants inoculated by the agar dish method, the lesion area was estimated by assuming a rectangular shape, and an elliptical shape was assumed for those inoculated by injection.

Lesion area data were used to estimate the area under the disease progress curve (AUDPC). AUDPC data were log-transformed for statistical analysis, assuming a randomized complete block design using SAS (version 8.2, SAS Institute Inc.). ANOVA was performed to detect differences between isolates, and the TUKEY test was run to evaluate statistically significant differences at $\alpha \leq 0.05$. The Kruskal Wallis and Dunn test was performed when normality and homogeneity assumptions were unmet.

Results

The disease occurred exclusively in *Rhizophora mangle* trees in the 13 plots where samples were gathered. Disease symptoms (galls and cankers) and signs (conidia, cirrus, pycnidia) were detected on prop roots and stems of *R. mangle* individuals at all developmental stages (seedlings, saplings, trees) (Fig. 2). A total of 80 samples of diseased tissue were collected from which 125 isolates were obtained and later classified into 24 morphotypes based on the macro and microscopic characteristics of the colonies. For the study, 42 isolates (n) representative of the most common morphotypes were chosen: Mph 1 (n = 10), Mph 2 (n = 9), Mph 3 (n = 12), Mph 6 (n = 2), Mph 21 (n = 4), and Mph 14 and 22 (n = 5).

Morphological and molecular identification

Based on morphological characteristics and molecular identification results from the ITS, TUB2, ACT, and EF1- α genes, the fungi identified include *Cytospora rhizophorae* (Mph 14 and 22), *Lasiodiplodia jatrophiicola*, and *L. theobromae* (Mph 3), *Rugonectria rugulosa* (Mph 21), as well as unidentified species from the genera *Fusarium* sp. (Mph 2), *Xenoacremonium* sp. (Mph 2), *X. recifei* (Mph 2) and *Clonostachys* sp. (Mph 6). Additionally, a novel group was classified within Cryphonectriaceae (Mph 1) (see Table 2).

Morphotype 1

Associated with stem galls and cankers on *Rhizophora mangle*. Asexual morphs on PDA. Pycnidia and conidia on sterilized pine needles on water agar (WA). *Pycnidia* globose, immersed, or semi-immersed, erumpent, either individual or grouped, dark brown to black, 170–1090 \times 110–1020 μ m in diameter, multilocular (Fig. 4D), delimited by dark lines, producing conidial mass, yellow or orange cirrus form (Fig. 4C). *Conidiophores* were short, filamentous in appearance, hyaline (Fig. 4E). *Conidia* hyaline, unicellular, elongated or curved and straight, with blunt ends, 3.7–5.9 \times 0.7–1.9 μ m (Fig. 4F).



Fig. 2 – Symptoms and signs of diseases. A. Galls. B. Stem Cankers. C and D. Cryphonectriaceae fungi sign, conidia cirrus.

Culture characteristics: Colonies with irregular edges, composed of mycelium that were olive gray or pale brown on the upper surface (Fig. 4A) and dark brown on the lower surfaces (Fig. 4B), had a plushy texture and a low presence of concentric rings. All isolates produced pycnidia and conidia on sterilized pine needles on WA after 20 days (Fig. 4C).

Material examined: Colombia, Urabá Golf, Antioquia, on *Rhizophora mangle*, living culture (Mph 1-1, Mph 1-2, Mph 1-3, Mph 1-4, Mph 1-5, Mph 1-6, Mph 1-7, Mph 1-8, Mph 1-9, Mph 1-10).

Notes – Fungal colonies identified as Mph 1 were found in 33.6% of the isolates obtained from diseased tissues (galls, cankers, and cirrus) collected in 10 plots dominated by *Rhizophora mangle* (red mangrove). Phylogenetic analysis based on combined ITS and TUB2 sequences, using

Maximum Likelihood (ML), Neighbor-Joining (NJ), and Bayesian Inference (BI) methods, produced a phylogenetic tree comprising 16 groups. Fifteen groups corresponded to known genera within Cryphonectriaceae, while Mph 1 isolates formed a separate group, representing an external lineage within the family. This separation was strongly supported by posterior probability values above 0.80 in the Bayesian Inference tree (Fig. 3) and bootstrap values over 80% in the ML and NJ analyses (data is not shown). The phylogenetic tree did not definitively place the Mph 1 isolates within an existing genus, suggesting that these fungi are likely to represent a new genus and species within Cryphonectriaceae. Further studies, including multigene analyses or genomic sequencing, are necessary to accurately determine their taxonomic position.

Most anamorphic species within the Cryphonectriaceae family exhibit orange or yellow conidiomata and/or ascomata. However, *Aurapex*, *Celoportha*, *Chrysophorthe*, and *Luteocirrhus* differ, producing dark brown to black pycnidia. This pigmentation pattern was also observed in the unidentified Cryphonectriaceae isolates of Mph 1. Mph 1 isolates showed a closer morphological resemblance to *Luteocirrhus*. Both groups form brown to black, pulvinate (cushion-shaped) to globose conidiomata, lacking necks (which are short and attenuated in *Luteocirrhus*). Their conidiomata are superficially positioned to semi-immersed and erumpent (superficial in *Luteocirrhus* but immersed in Mph 1). These conidiomata are ostiolate, meaning they have small openings, and are either uni- or multilocular. The conidiophores are hyaline and filamentous, and their conidia are also hyaline, aseptate, straight or slightly curved (allantoid), and exude in the form of orange cirrus or yellow droplets. Sexual reproductive structures were absent in both Mph 1 and *Luteocirrhus*.

Morphotype 2

Associated with stem galls and cankers on *Rhizophora mangle*. Asexual morphs on APDA. Morphological description of Mph 2-1, 2-2, 2-3, 2-5, 2-8 and 2-11 (Lombard et al. 2015): Conidial with mycelium grown on APDA. Colonies with filamentous edges composed of septate, hyaline mycelium, pale yellow or pink on the upper and lower surfaces), with plushy texture and low presence of cottony sectors (Fig. 6A). All isolates produced septate and hyaline mycelium; whorled conidiophores arise from somatic hyphae (Fig. 6D). Spore masses formed loose to compact heads (Fig. 6E). *Conidia* hyaline, single-celled, slightly curved, with blunt to pointed ends, 2.4–7.5 μm long \times 0.9–3.2 μm wide (Fig. 6C).

Morphological description of Mph 2-6 (Lombard et al. 2014): Conidial with mycelium grown on APDA. Colony with filamentous edges, white with a slightly cottony to powdered texture, center with pale yellow upper and lower surface, septate mycelium, with the presence of sectors (Fig. 7A). Unicellular, hyaline, slightly curved conidia (Fig. 7B). Conidiophore simple and short (Fig. 7C).

Morphological description of Mph 2-14 and Mph 2-4 (Lombard et al. 2015): Conidial with mycelium grown on APDA. Colony with a filamentous edge, plush texture, pale yellow edge of the upper and lower face and yellow towards the center, without formation of sectors (Fig. 6B). Mycelium septate, hyaline and whorled conidiophores (Fig. 6D), conidia hyaline without septation, curved to slightly curved (Fig. 6C), loose or in compact masses (Fig. 6E).

Material examined: Colombia, Urabá Gulf, Antioquia, on *Rhizophora mangle*, living culture (Mph 2-1, Mph 2-2, Mph 2-3, Mph 2-4, Mph 2-5, Mph 2-6, Mph 2-8, Mph 2-11, Mph 2-14).

Notes – Fungal colonies corresponding to Mph 2 were detected in 13.6% of isolates from diseased tissues, including galls, cankers, and cirrus, collected from 11 plots. Morphological analysis identified three colony types, which did not necessarily correspond to the genera and/or species identified at the molecular level. Although strains Mph 2-4 and Mph 2-14 were molecularly identified as *Xenoacremonium recifei*, they exhibited differences in colony morphology.

Phylogenetic analysis of Mph 2 isolates, based on combined ITS and TUB2 consensus sequences using both Neighbor-Joining (NJ) and Maximum Likelihood (ML) analyses, grouped the isolates into the genera *Xenoacremonium* (eight isolates: six as an unidentified species and two as *X. recifei*) and *Fusarium* (one isolate) (Fig. 5), corroborating their morphological identification (Fig.5).

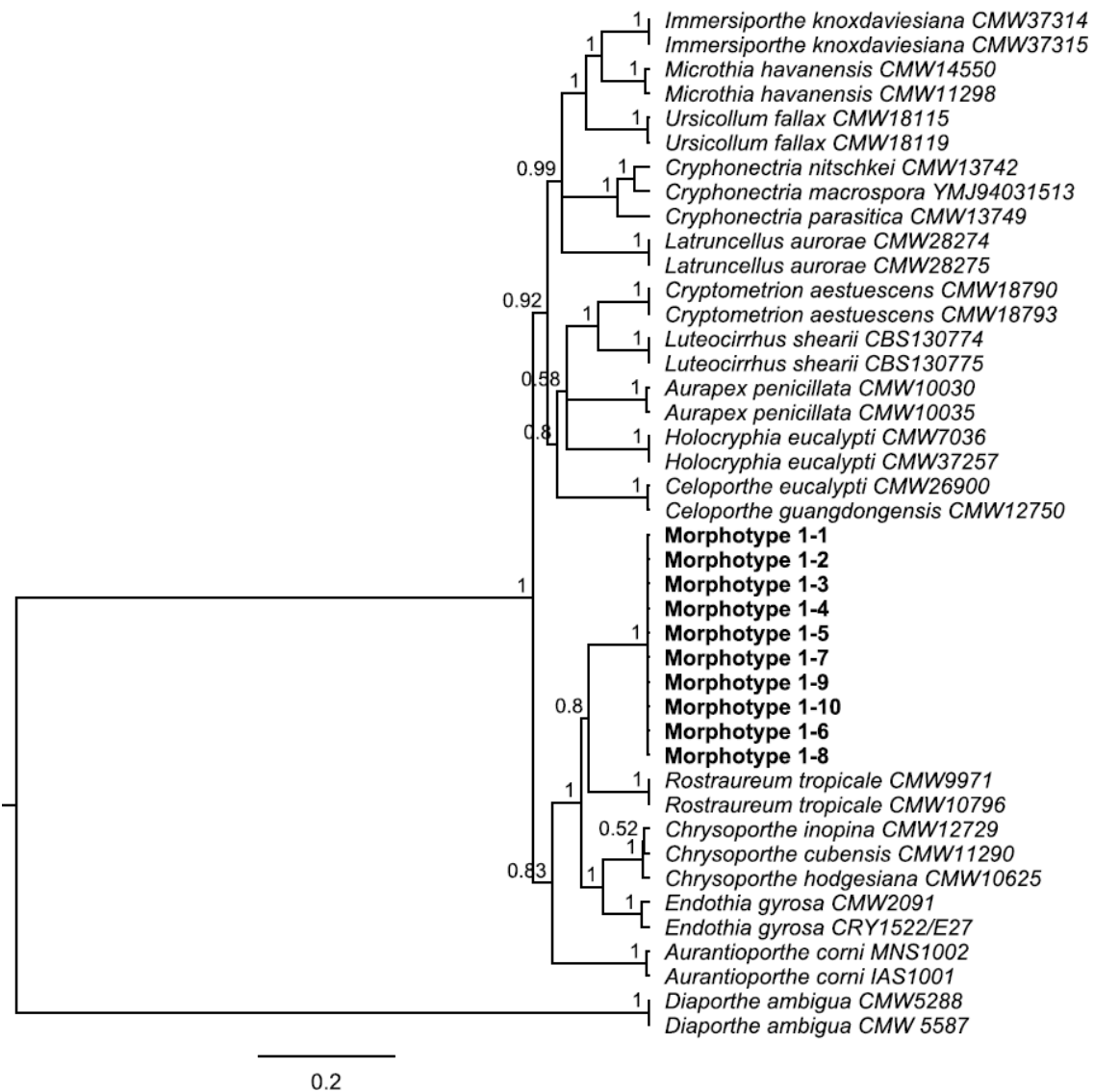


Fig. 3 – The phylogenetic tree generated from Bayesian inference (BI) analysis based on combined ITS and TUB2 sequence data from 42 strains of Cryphonectriaceae. The tree is rooted to *Diaporthe ambigua* strains CMW5288 and CMW5587. Bayesian posterior probability values are given at the nodes in this order. The Morphotype -1 isolates in this study appear bold.

The morphology of the eight Mph 2 isolates grouped with *Xenoacremonium* (Mph 2-1, Mph 2-2, Mph 2-3, Mph 2-4, Mph 2-5, Mph 2-8, Mph 2-11, and Mph 2-14) displayed septate, hyaline mycelium with whorled conidiophores emerging from somatic hyphae. Spore masses developed into loose to compact heads, and the conidia were single-celled, slightly curved, hyaline, with blunt to pointed ends (Figs. 6). These morphological characteristics were consistent with the descriptions of *Xenoacremonium* provided by Lombard et al. (2015). Accordingly, these eight isolates were identified as *Xenoacremonium* sp. and *X. recifei*.

Additionally, one isolate from Mph 2 (Mph 2-6) exhibited morphological features consistent with cotton-like colonies, with a slight pink tinge towards the centre and formation of sectors. Conidiophores are simple, short, microconidia hyaline, unicellular, oblong or slightly curved. These characteristics matched descriptions of *Fusarium* sp. (Fig. 7).

Morphotype 3

Associated with stem galls and cankers on *Rhizophora mangle*. Asexual morphs on APDA. Pycnidia and conidia on sterilized pine needles in WA. Morphological description of Mph 3-1, 3-2,

3-3, 3-4, 3-5, 3-7, 3-8, 3-9, 3-10, 3-11, and 3-12. Colonies are dark grayish brown, with velvety texture and solid border. Sectors and fruiting bodies absent (Fig.9A). *Pycnidia* were globose, dark brown to black, single, or grouped covered with white to grey mycelium, $108.9\text{--}997.1 \times 108.5\text{--}999.1 \mu\text{m}$. *Conidia* were hyaline, double-walled when young, later becoming dark brown with longitudinal striations and 1-septum, $12.2\text{--}28.6 \mu\text{m}$ long \times $8.0\text{--}19. \mu\text{m}$ wide (Fig.9B).

Morphological description of Mph 3-6. Colony white to light gray, gray and dark gray toward the center, texture cottony to velvety, aerial mycelial masses of fruiting body primordia (Fig. 10A and 10B). *Pycnidia* were globose, dark brown to black, single, or grouped covered with white to grey mycelium, $200.31 \times 682.42 \mu\text{m}$ long \times $187.72 \times 635.03 \mu\text{m}$ wide (Fig. 10C). *Conidia* were hyaline, double-walled when young (Fig.10D), later becoming dark brown with longitudinal striations and 1-septum, $14.17 - 28.51 \mu\text{m}$ long \times $9.39\text{--}14.61 \mu\text{m}$ wide (Fig. 10E), (scale bar $100 \mu\text{m}$).

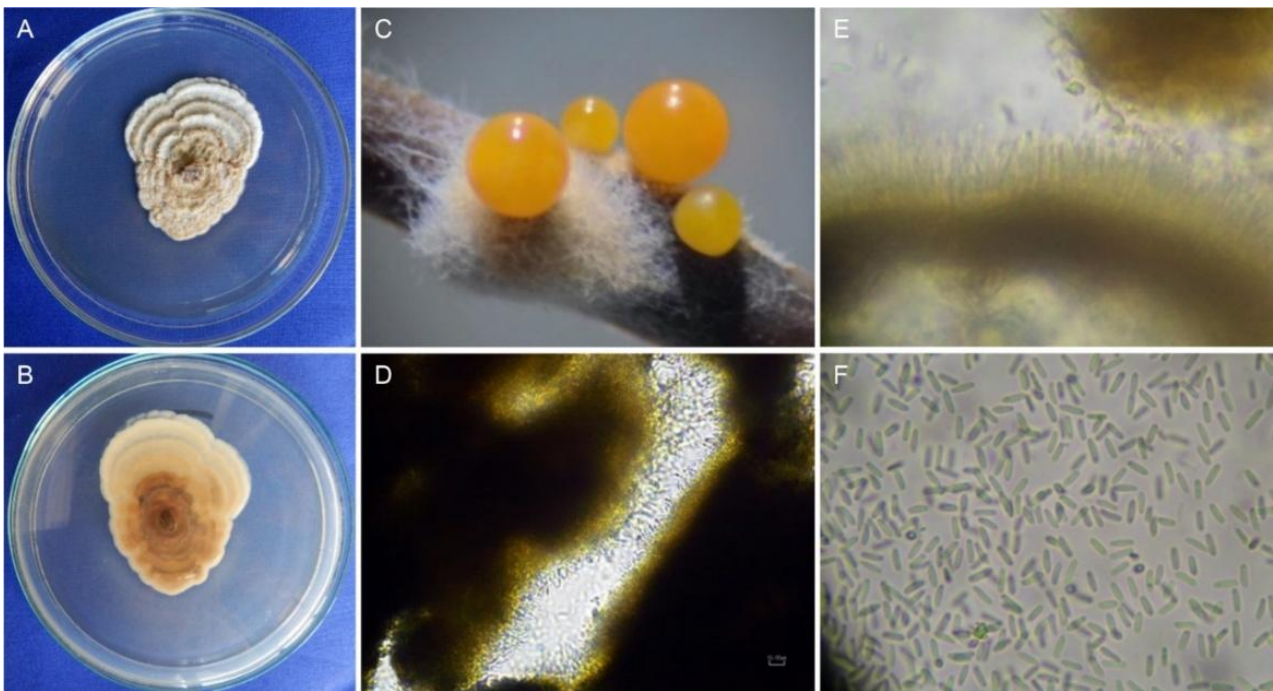


Fig. 4 – Morphotype 1: A and B. Colony on APDA (A: upper face; B: lower face). C. Pycnidium on pine needles oozing conidia. D. Immersed conidioma horizontal section showing multiple locules. E. Unicellular hyaline conidiophores. F. Unicellular conidia.

Culture characteristics: Colonies with uniform edges, composed of mycelia that were very dark gray black on the upper surfaces (Fig.9A) and black on the lower surfaces, with cottony texture and low presence of mycelia aggregates of immature pycnidia (Figs.9A). All isolates produced pycnidia and conidia on sterilized pine needles on WA after 20 days.

Material examined: Colombia, Urabá Gulf, Antioquia on *Rhizophora mangle*, living culture (Mph 3-1, Mph 3-2, Mph 3-3, Mph 3-4, Mph 3-5, Mph 3-6, Mph 3-7, Mph 3-8, Mph 3-9, Mph 3-10, Mph 3-11, Mph 3-12).

Table 2 Morphological characteristics described for fungi isolated from gall and canker tissues of *R. mangle*.

Morphotype	Taxon name	Colony			Conidiomata			Conidia			Growth rate range (mm/d)
		Type ¹	Color ²		Type	Long μ m	Width μ m	Type	Long μ m	Width μ m	
			UF	LF							
1	Chryphonectriaceae	A, B, C	Olive gray or pale brown	Dark brown	Dark brown to black pycnidia immersed or semi-immersed globose erumpents	170–1090.4	109.5–1020.8	Single-celled. Hyaline Elongated Slightly curved	3,7–5,9	0,7–1,9	2,2–4,7
2	<i>Fusarium</i> sp. (2-6)	B	Pale yellow or pink	Pale yellow or pink	-	-	-	Unicellular Hyaline slightly curved Moonlike forming conidial heads	2.4–7.5	0.9–3.2	2,38–3,6
	<i>Xenoacremonium</i> sp. (2-1, 2-2, 2-3, 2-5, 2-8, 2-11)	B	Pale yellow and pink	Pale yellow and pink	-	-	-		4.84 – 9.82	2.33 – 4.83	
	<i>X. recifei</i> (2-4, 2-14)	B	Pale yellow and yellow	Pale yellow and yellow	-	-	-		3,54 – 6,69	0,91 – 2,32	
3	<i>Lasiodiplodia jatrohicola</i>	A, B	Dark greyish brown and black	Black	Dark brown to black pycnidia shallow individual or grouped	108,9–997,1	108,5–999,1	Hyaline and unicellular conidia in immature state.	12,2–28,6	8,0–19	5,7–24,3
	<i>L. theobromae</i>	A	Dark greyish brown	Black		200.31 – 682.42	187.72 – 635.03	Mature conidia had a central septum, pale brown to dark color and longitudinal striations.	14,17 – 28,51	9,39 – 14,61	

Table 2 Continued.

Morphotype	Taxon name	Colony			Conidiomata			Conidia			Growth rate range (mm/d)
		Type ¹	Color ²		Type	Long μm	Width μm	Type	Long μm	Width μm	
			UF	LF							
6	<i>Clonostachys</i> sp.	B	Pinkish white	Pink	–	–	–	Unicellular subhyaline Ovoid to elongated	3,1–6,1	1,6–2,2	2,7–3
21	<i>Rugonectria rugulosa</i>	B	Rings in Beige, Reddish Yellow, and Pale Brown Colors	Reddish yellow	–	–	–	Microconidia: uni and bicellular hyaline, ellipsoid to cylindrical and slightly curved. Macroconidia: smooth, straight or slightly curved, with two to three septa	3,0–15,2	1,6–5,5 4,5–5,0	3,5–4,2
14 and 22	<i>Cytospora rhizophorae</i>	B	Rings of pale brown to dark brown. Sometimes whole beige	Pale brown to dark brown	Pycnidia semi-immersed to superficial, globose, erumpent	293,1–693,5	188,5–838,4	Single-celled hyaline elongated slightly curved	2,9–6,6	0,6–1,7	3,1–4,7

¹ Colony type. A: Irregular shape, filamentary edge and plush texture; B: Circular shape, filamentary edge, plush texture; C: Circular shape, filamentary edge, plush texture and concentric rings

² Colony color. UF: upper face, LF: lower face

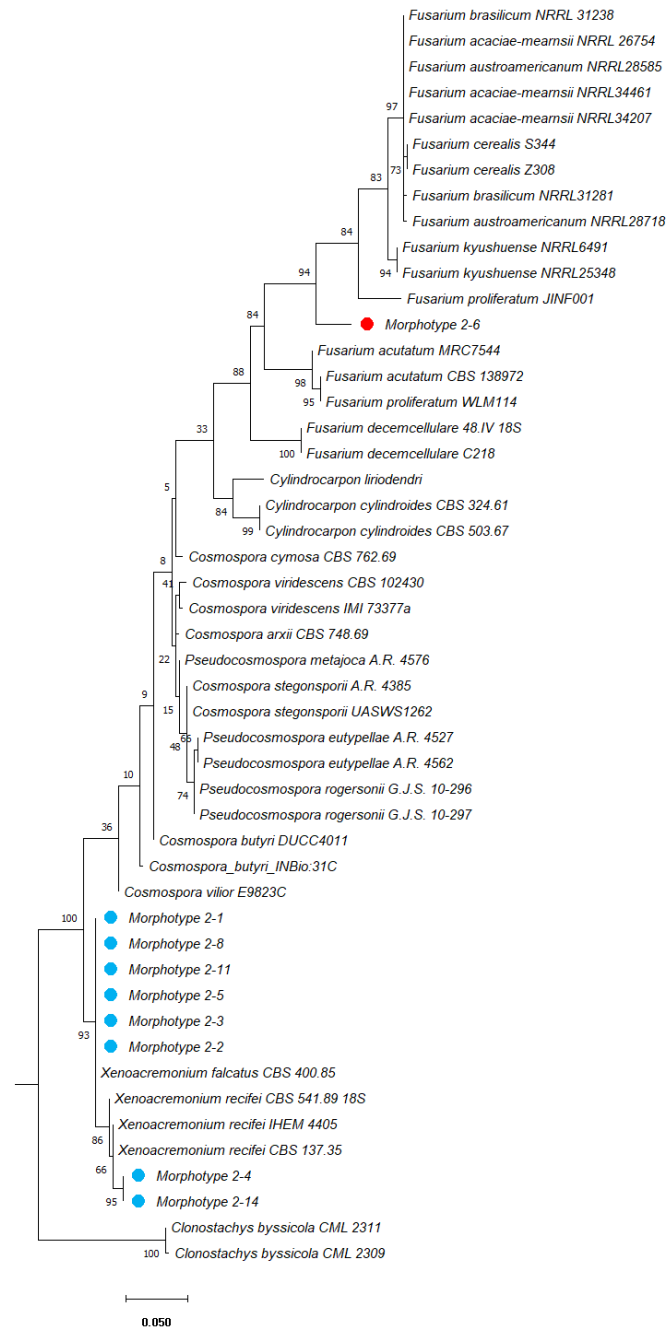


Fig. 5 – Phylogenetic tree generated from maximum likelihood (ML) analysis based on ITS sequence data from 49 strains of the *Xenoacremonium*, *Fusarium*, and closed genera. The tree is rooted to *Clonostachys byssicola* strain CML 2311 and CML 2309. Maximum likelihood bootstrap values are given at the nodes. The red and blue circle was mentioned before the species in this study.

Notes – Colonies corresponding to Mph 3 were identified in 14.4% of isolates collected from diseased tissues (galls, cankers, and cirrus) across eight vegetation plots. Phylogenetic analysis of the ITS region and TUB2, and EF1- α genes for Mph 3 isolates, using Maximum Likelihood (ML) and Neighbor-Joining (NJ) methods, grouped these fungi with species of *Lasiodiplodia*. The phylogenetic trees resolved eight groups representing seven species of *Lasiodiplodia* genus and the species *Spencermartinsia viticola* as the outgroup (Fig. 8). Eleven isolates (Mph 3-1, Mph 3-2, Mph 3-3, Mph 3-4, Mph 3-5, Mph 3-6, Mph 3-7, Mph 3-8, Mph 3-9, Mph 3-10, Mph 3-11, and Mph 3-12) were grouped within the species *Lasiodiplodia jatrophiicola* and therefore were identified as *L. jatrophiicola*, while one isolate (Mph 3-6) was placed in the species *L. theobromae* and identified

as *L. theobromae* (Fig. 8). Molecular identification using combined ITS and EF1- α sequence analysis further confirmed the classification of Mph 3 isolates as *L. jatrophiicola* and *L. theobromae* (Fig. 8). Based on morphological characteristics and phylogenetic analyses, eleven red mangrove isolates were identified as *L. jatrophiicola* (Mph 3-1, Mph 3-2, Mph 3-3, Mph 3-4, Mph 3-5, Mph 3-7, Mph 3-8, Mph 3-9, Mph 3-10, Mph 3-11, and Mph 3-12), while one isolate (Mph 3-6) was confirmed as *L. theobromae* (Phillips et al. 2013).

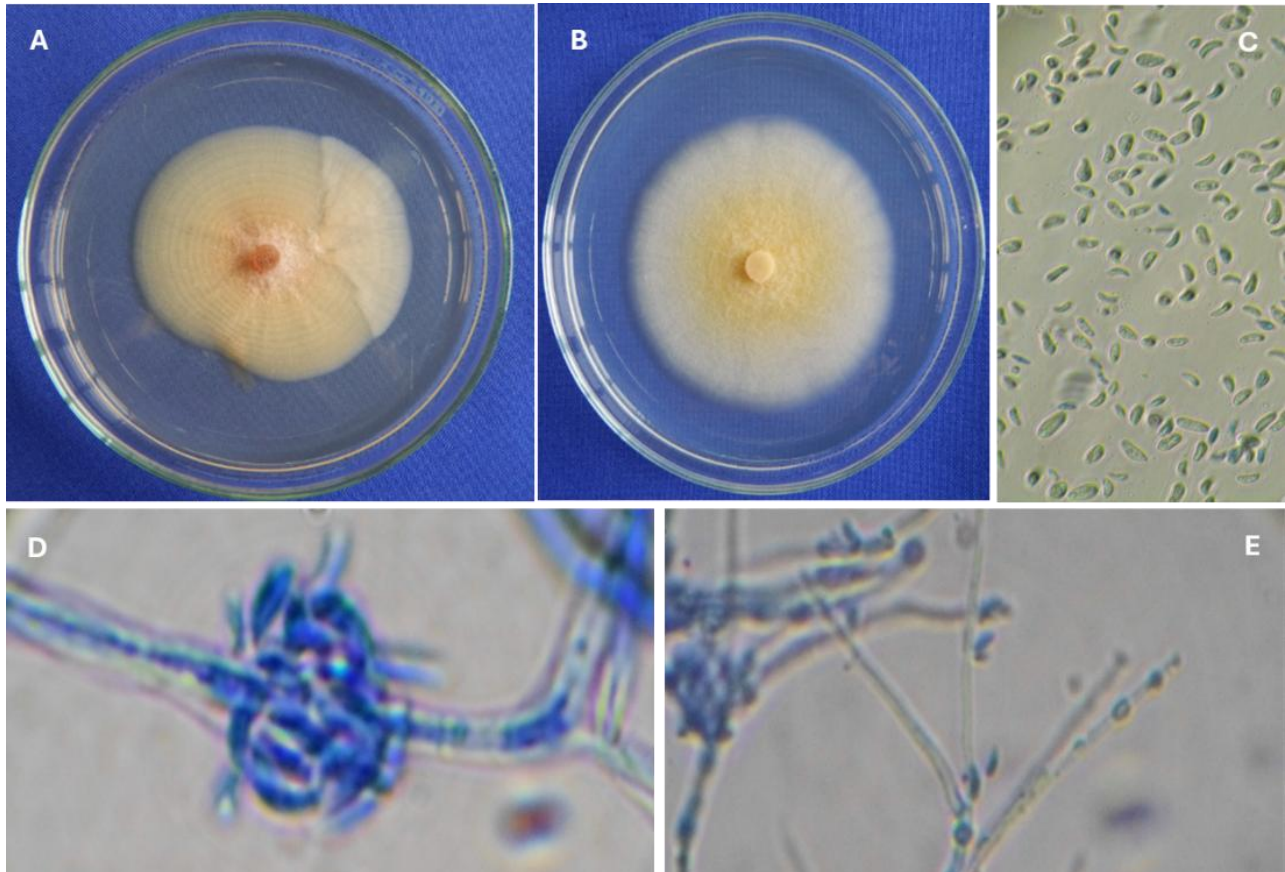


Fig. 6 – Morphotype 2 (Mph 2-1, Mph 2-2, Mph 2-3, Mph 2-4, Mph 2-5, Mph 2-8, Mph 2-11): A. Colony on APDA showing upper face for Mph 2-1, Mph 2-2, Mph 2-3, Mph 2-5, Mph 2-8 and Mph 2-11. B. Colony on APDA showing upper face for Mph 2-4 and 2-14. C. Unicellular, hyaline, slightly curved conidia. D. Spindle-shaped conidia forming false heads. E. Verticillate conidiophores arising laterally from somatic hyphae.

Morphotype 6

Associated with stem galls and cankers of *Rhizophora mangle*. Asexual morphs on PDA. Mycelium and conidia on PDA, produced hyaline septate hyphae, vertically branched conidiophores (Fig. 12C), and conidial masses formed gelatinous heads (Fig. 12D). Conidia were sub-hyaline, single-celled, ovoid to elongated, $3.1\text{--}6.1 \times 1.6\text{--}2.2 \mu\text{m}$ (Fig. 12E).

Culture characteristics: Colonies with pinkish white mycelium on the upper surface (Fig. 12A) and pink lower surface (Fig. 12B), with fluffy texture and cottony sectors.

Material examined: Colombia Urabá Gulf, Antioquia on *Rhizophora mangle*, living culture (Mph 6-1, Mph 6-2).

Notes – Fungal colonies identified as Mph 6 were observed in 1.6% of isolates collected from spore cirrus within a singular vegetation plot. Phylogenetic analysis of the Internal Transcribed Spacer (ITS) region, using the Maximum Likelihood (ML) method, delineated seven well-supported groups. That corresponded to the genera *Geosmithia*, *Stromatonectria*, *Gliomastix*, *Clonostachys*, *Fusarium*, *Heleococcum*, and *Ovicillium attenuatum*, respectively, with the latter serving as the

outgroup (Fig. 11). The two Mph 6 isolates were classified within species of *Clonostachys*, substantiated by a bootstrap value of 97%. Therefore, based on morphological characteristics and phylogenetic analyses, the Mph 6 isolates were identified as *Clonostachys* sp.

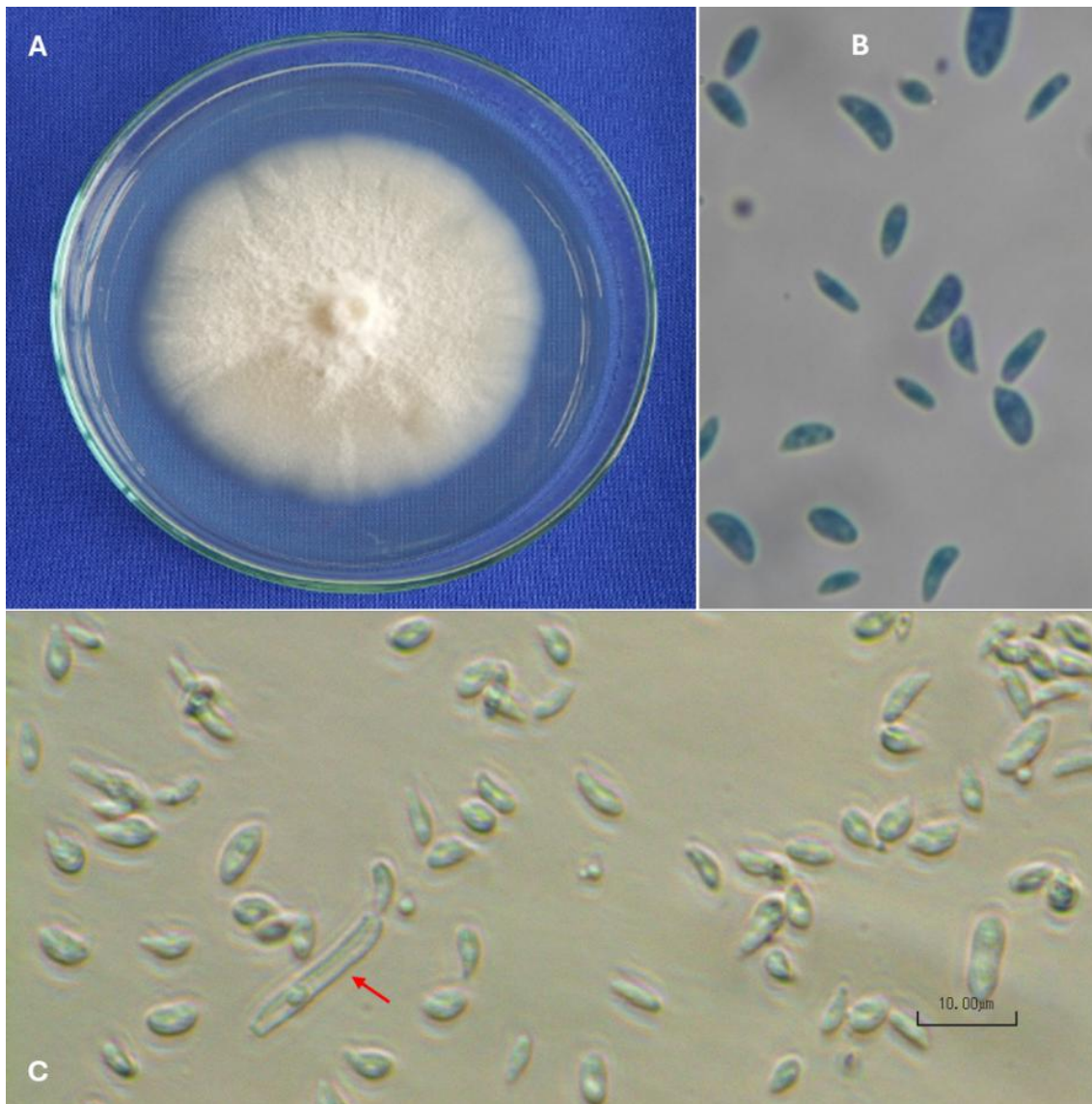


Fig. 7 – Morphotype 2 (Mph 2-6): A. Colony on APDA medium showing upper face for Mph 2-6. B and C. Unicellular, hyaline, slightly curved microconidia, simple, short conidiophore (arrow). Scale bar 10 μ m.

Morphotype 21

Associated with stem galls and cankers on *Rhizophora mangle*. Asexual morphs on PDA. Mycelium and conidia on PDA. Micro and macroconidia were present. Microconidia were hyaline and ellipsoid, with one to 2-septa (Fig. 14C). Other shapes were cylindrical and slightly curved, with rounded ends, $3.0\text{--}15.2 \times 1.6\text{--}5.5 \mu\text{m}$. Macroconidia were smooth, straight or slightly curved, with two to 3-septa and blunt ends, $32.8\text{--}56.2 \times 4.5\text{--}5.0 \mu\text{m}$ (Fig.14D). These morphological characteristics were like those described for the genus *Rugonectria*.

Culture characteristics: Colonies with filamentous edges, composed of beige or reddish yellow mycelium on the upper surface and reddish yellow on the lower surface (Figs. 14A and 14B), with plushy texture and low presence of concentric rings. Most isolates produced septate hyphae.

Material examined: Colombia, Urabá Gulf, Antioquia on *Rhizophora mangle*, living culture (Mph 21-1, Mph 21-2, Mph 21-3, Mph 21-4).

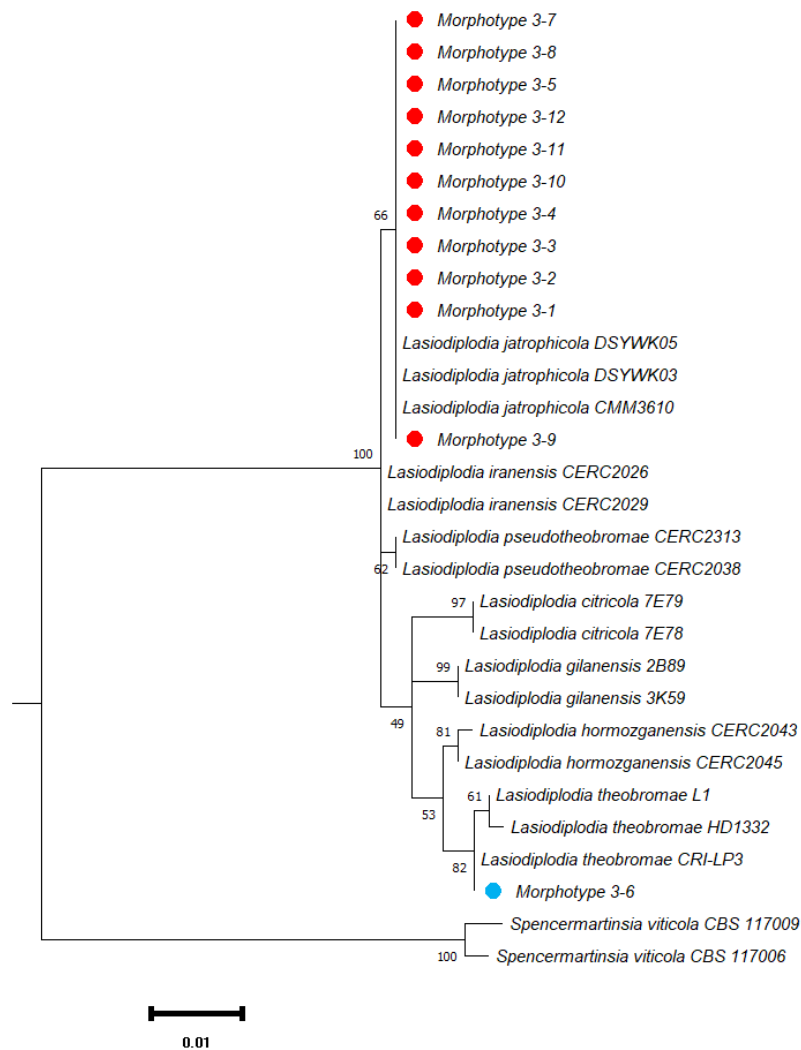


Fig. 8 – Phylogenetic tree was generated from maximum likelihood (ML) analysis based on combined ITS and TUB2 sequence data from 30 strains of *Lasiodiplodia*. The tree is rooted to *Spencermartinsia viticola* strains CBS 117009 and CBS 117006. Maximum likelihood bootstrap values are given at the nodes in this order. The red and blue circle was mentioned before the species in this study.

Notes – Fungal colonies of Mph 21 were found in 3.2% of isolates obtained from diseased tissues collected in three vegetation plots. Phylogenetic analysis of the ITS region and EF1- α gene, using the Maximum Likelihood (ML) method, resolved seven groups with strong bootstrap support. The groups corresponded to *Rugonectria rugulosa*, *Rugonectria castaneicola*, *Ilyonectria macrodidyma*, *Nectria balsamea*, *Nectria pseudotrichia*, *Stromatonectria caraganae*, and *Neonectria major*, respectively. The four mangrove isolates of Mph 21 were grouped within the species *Rugonectria rugulosa*, with high bootstrap support of 92% (Fig. 13). Hence, based on morphological characteristics (Chaverri et al. 2011) and phylogenetic analyses, the four isolates of Mph 21 were identified as *Rugonectria rugulosa*.

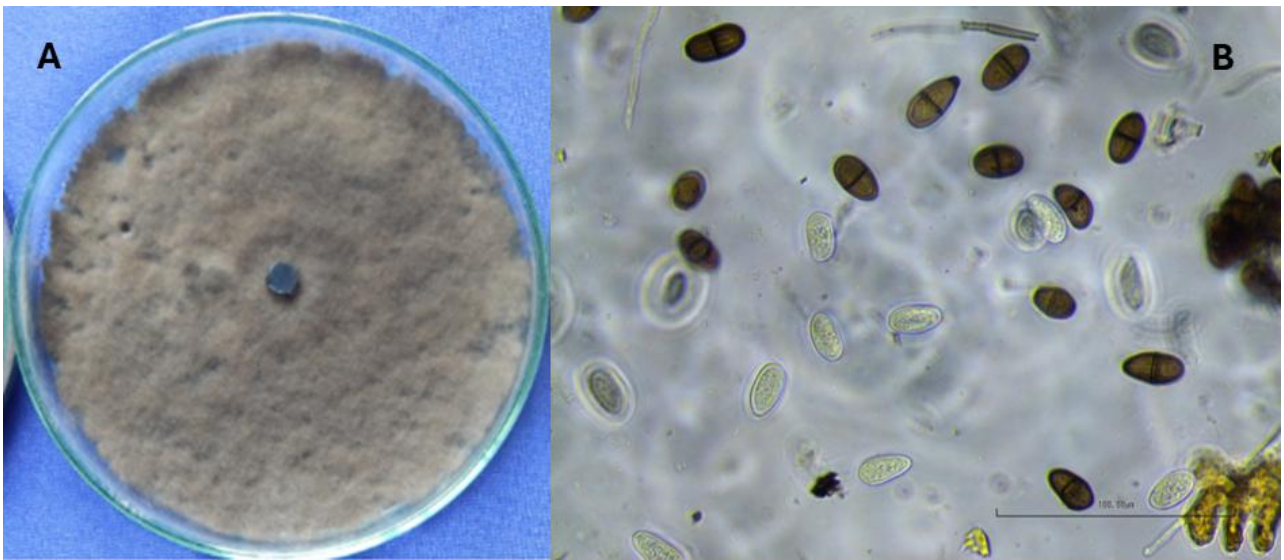


Fig. 9 – Morphotype 3 (Mph 3-1, 3-2, 3-3, 3-4, 3-5, 3-7, 3-8, 3-9, 3-10, 3-11 and 3-12): A. colony on APDA showing upper face. B. Immature hyaline aseptate conidia; mature dark brown conidia with central septum and striations. Scale bar 100 µm.

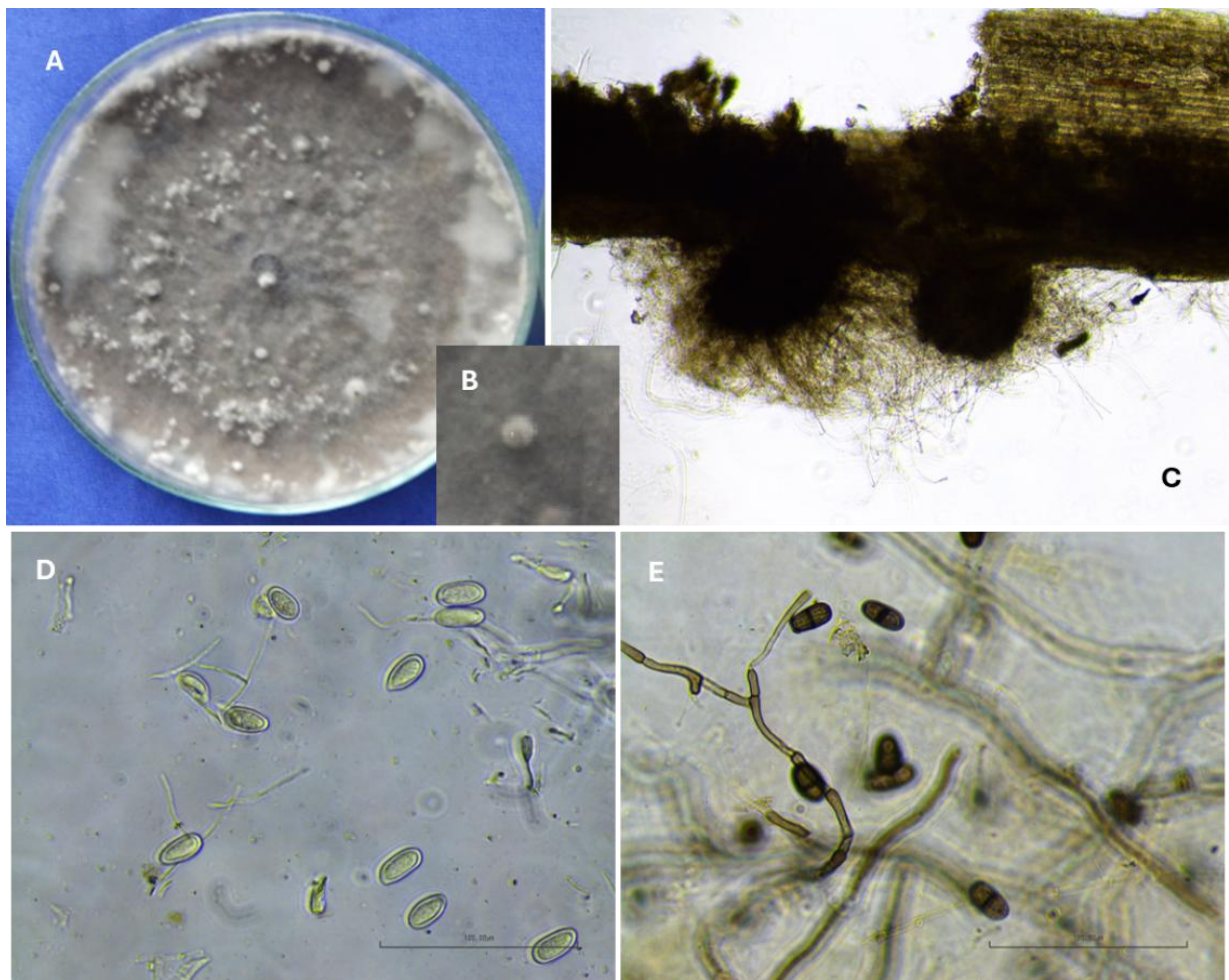


Fig. 10 – Morphotype 3 (Mph 3-6): A. Colony on APDA showing upper face. B. Mycelia aggregate of immature pycnidia. C. Pycnidium with aerial mycelium on pine needle. D. Immature, hyaline conidia aseptate. E. Mature, dark brown conidia with central septum. Scala bar 100 µm.

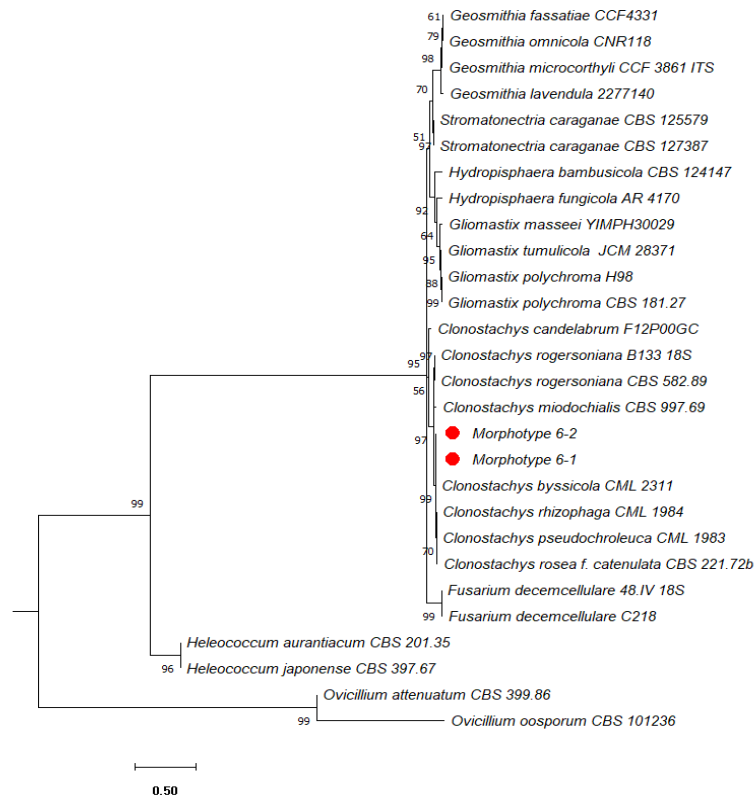


Fig. 11 – Phylogenetic tree generated from maximum likelihood analysis based on ITS sequence data from 28 strains of *Clonostachys* and close genera. The tree is rooted to *Ovicillium attenuatum* strain CBS 39.86 and *O. oosporum* CBS 101236. Maximum likelihood bootstrap values are given at the nodes in this order. The red circle was mentioned before the species in this study.

Morphotypes 14 and 22

Associated with stem galls and cankers on *Rhizophora mangle*. Asexual morph on PDA. Pycnidia and conidia on sterilized pine needles in WA. Pycnidia 293.12–693.47 × 188.51–838.44 μm, globose, semi-immersed or superficial, erumpent, individual or grouped, dark brown, with conidial mass; conidial mass yellow drops (Fig. 16D). Conidiophores were short, hyaline, and filamentous appearing (Fig. 16C). Conidia 3–7 × 1–2 μm elongated and curved with blunt ends, hyaline, with 1-septum. These morphological characteristics were like those described for the genus *Cytospora*.

Culture characteristics: Morphotypes 14 and 22 colonies with filamentous edges, composed of pale to dark brown mycelium on the upper surface (Fig. 16A) and yellow orange to dark brown on the lower surface (Fig. 16B), with a fluffy texture. Most isolates produced pycnidia and conidia on sterilized pine needles on WA after 25 days (Fig. 16D).

Material examined: Colombia, Urabá Gulf, Antioquia, on *Rhizophora mangle*, living culture (Mph 14-1, Mph 14-2, Mph 22-1, Mph 22-2, Mph 22-3).

Notes – Colonies of Mph 14 and 22 were found in 3.2% of isolates obtained from diseased tissues (galls, cankers, and cirrus) collected across four vegetation plots. Phylogenetic analysis of the ITS region using Maximum Likelihood (ML) methods yielded a tree with eight groups. All mangrove isolates associated with *C. rhizophorae*, while the other four groups represented the species *C. abyssinica*, *C. variostromontana*, *C. leucostoma*, *C. chrysosperma*, *C. disciformis*, *C. eucalypticola*, and *C. diatrypelloidea*, respectively. Two strains of *Phomopsis bougainvilleicola* appear as an outgroup. The five isolates from Mph 14 and 22 are grouped with *C. rhizophorae* (Fig. 15). Therefore, based on morphological characteristics (Adams & Winfield 2006) and phylogenetic analyses, the five isolates from Mph 14 and 22 were identified as *Cytospora rhizophorae*.

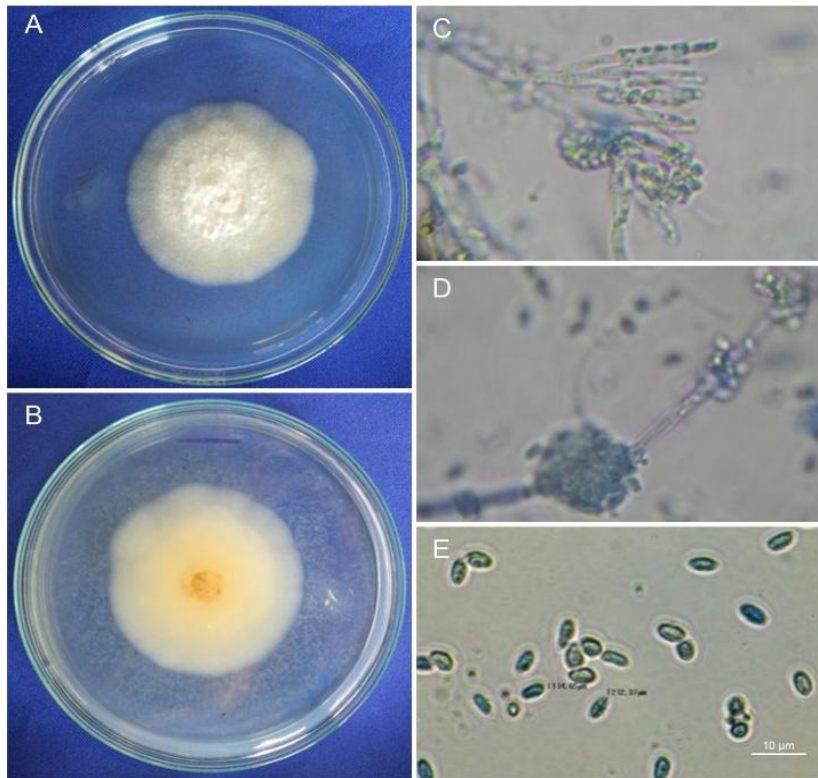


Fig. 12 – Morphotype 6. A. Colony on PDA upper face. B. Colony lower face. C. Verticillate conidiophores. D. Conidiophores producing conidial heads. E. Loose conidia. Scale bar: 10 µm.

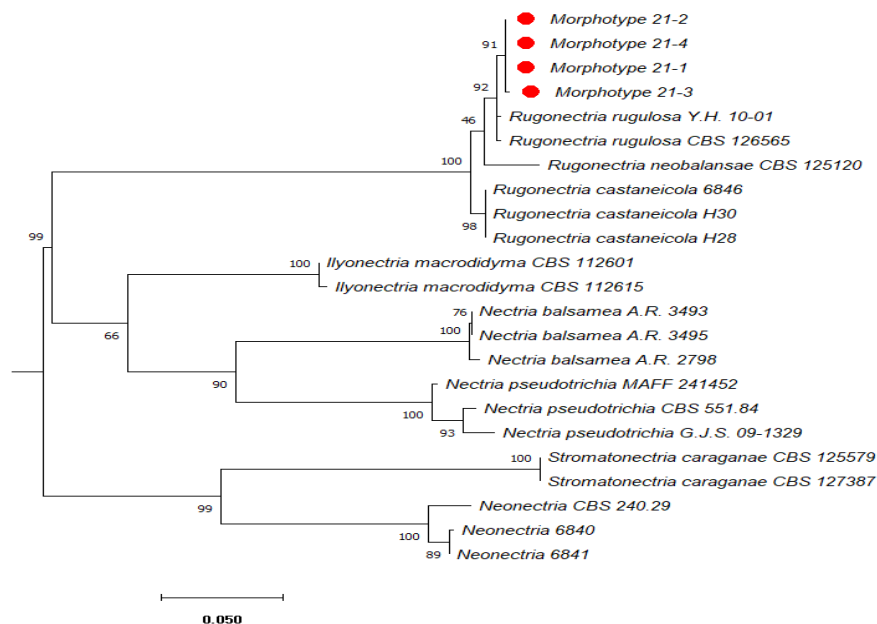


Fig. 13 – Phylogenetic tree was generated from maximum likelihood analysis based on combined ITS and EF1- α sequence data from 23 strains of *Rugonectria* and close genera. Maximum likelihood bootstrap values are given at the nodes in this order. The red circle was mentioned before the species in this study

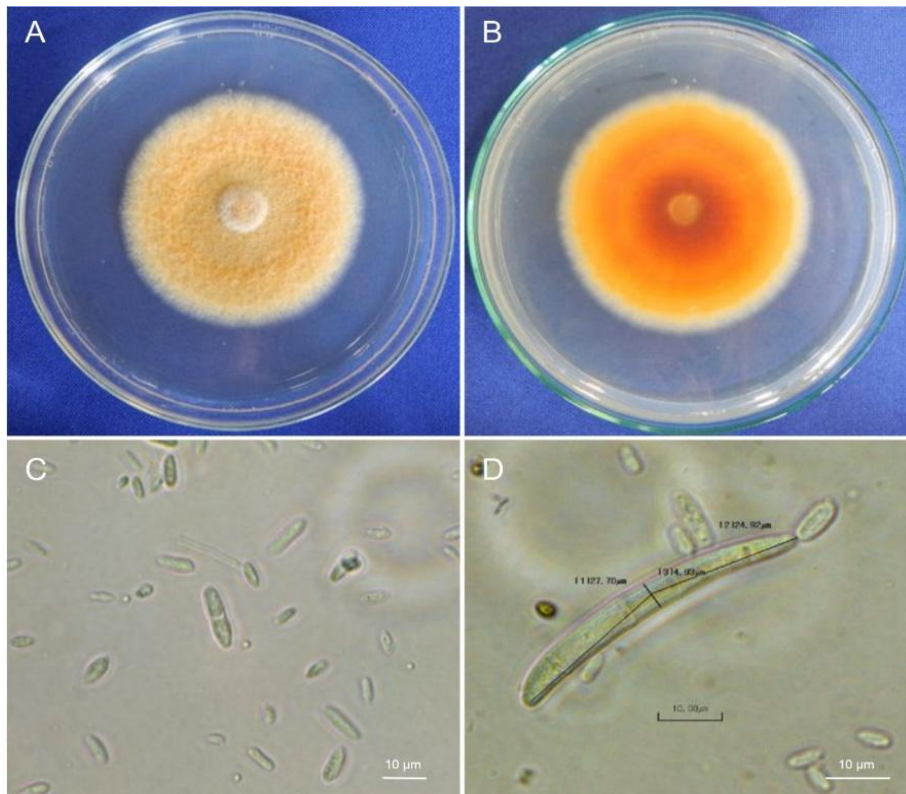


Fig. 14 – Morphotype 21. A. Colony on PDA upper face. B. Colony on PDA lower face. C. Microconidia. D. Macroconidia (scale bar 10 μm).

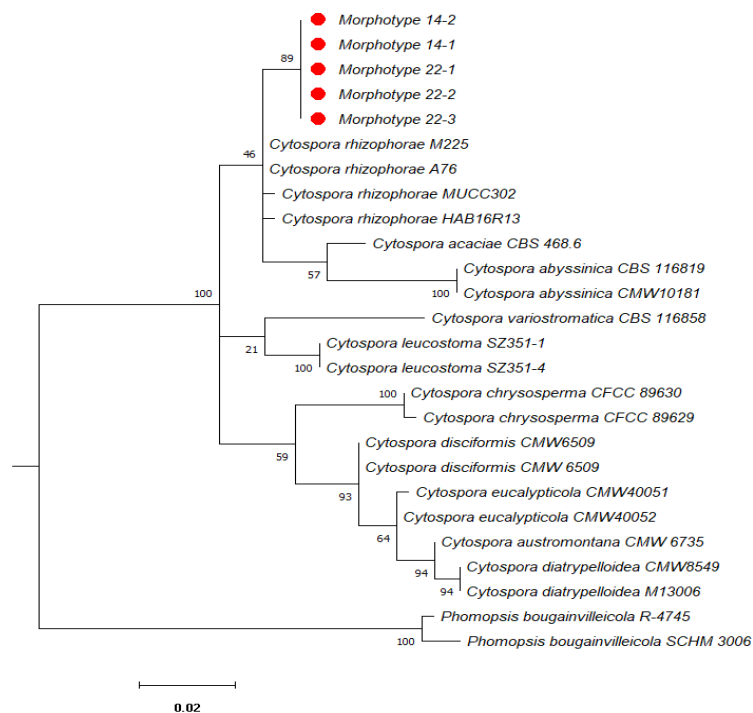


Fig. 15 – Phylogenetic tree generated from maximum likelihood analysis based on ITS sequence data from 26 strains of *Cytospora*. The tree is rooted to *Phomopsis bougainvilleicola* strain R-4745 and SCHM 3006. Maximum likelihood bootstrap values are given at the nodes in this order. The red circle was mentioned before the species in this study.

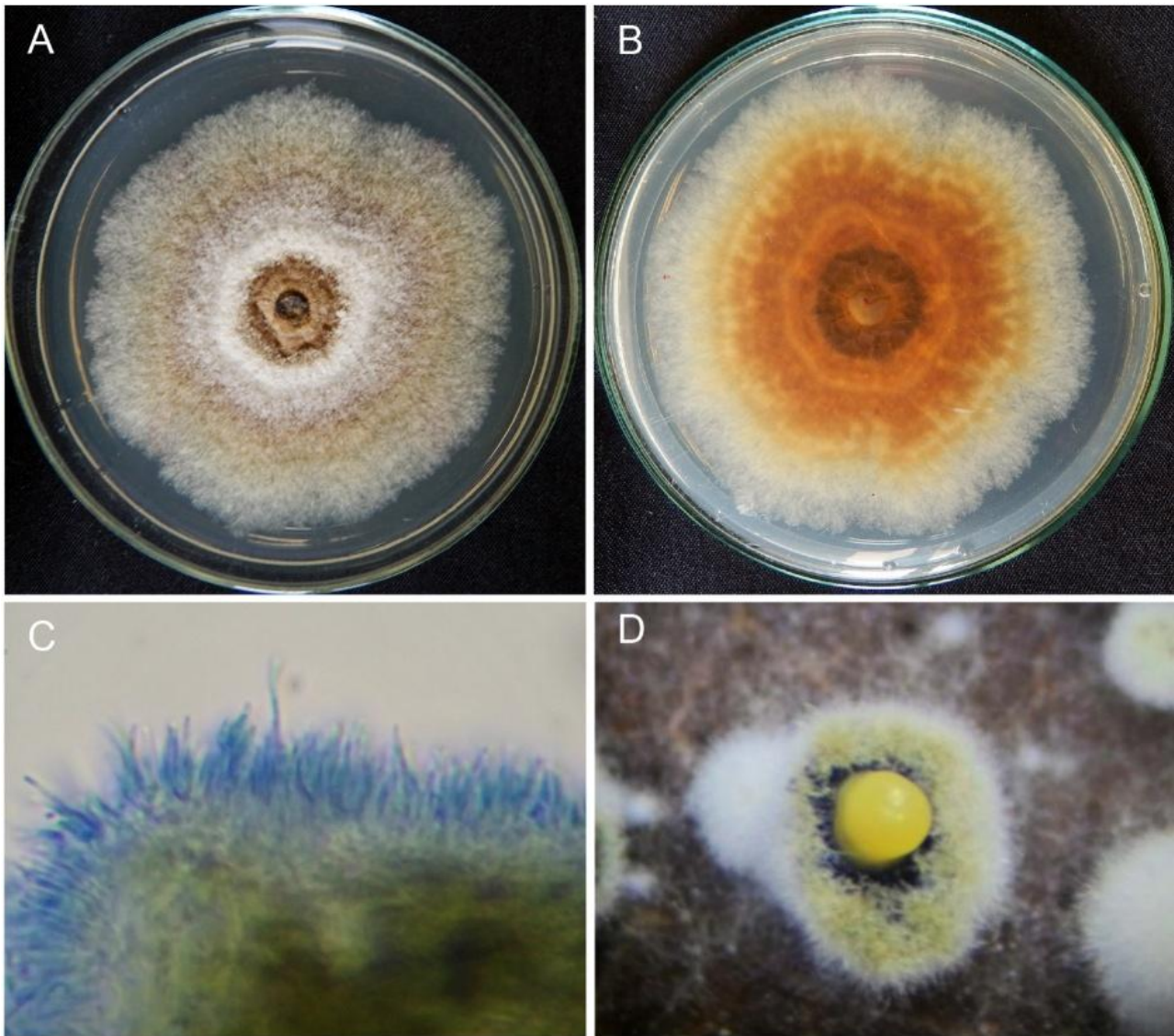


Fig. 16 – Morphotypes 14 and 22. A, B. Colony on PDA (A: upper, B: lower). C. Hyaline conidiophores. D. Pycnidium on eucalyptus leaf oozing yellow conidia mass.

Pathogenicity tests

Results of the pathogenicity field assays showed statistically significant differences only in plants inoculated with conidia suspension of Cryphonectriaceae (Treatment 3). Plants undergoing this treatment developed deep canker-like lesions 30 weeks after inoculations. The lesion size was measured 42.16 mm long by 14.33 mm wide and had an AUDPC of 3210.9, compared with a mean AUDPC of 1780.6 (Fig. 17-1). The control plant and those submitted to other inoculation treatments showed bulging lesions or scars restricted to the inoculation point (Fig. 17-2).

Data obtained from greenhouse inoculation did not meet the assumption normality and homogeneity of variance and, therefore, was analyzed with the Kruskal-Wallis test. Results showed significant differences across at least two treatments. Comparisons between treatments using the Dunn test showed significant differences in AUDPC between T1 (control) and T5 ($P < 0.0066$) and between T2 and T10 ($P < 0.0336$) (Fig. 18-1). Mph 1 and Mph 3 isolates were the most aggressive ones. The plants inoculated with *Lasiodiplodia* spp. died and some developed necrotic lesions on stems, with average dimensions of 18×7.5 mm (Figs. 18-2E, 18-2F).

Plants inoculated with the species of Cryphonectriaceae developed chlorotic halos around the lenticel, followed by slight necrosis, bulging and callus formation. Lesions were 7×6.3 mm (Fig.

18-2C.). Plants with simultaneous inoculation of these two fungi showed early development of disease symptoms, with stem necrosis on week 1 followed by plant death on week 2 after inoculation (Fig. 18-2D).

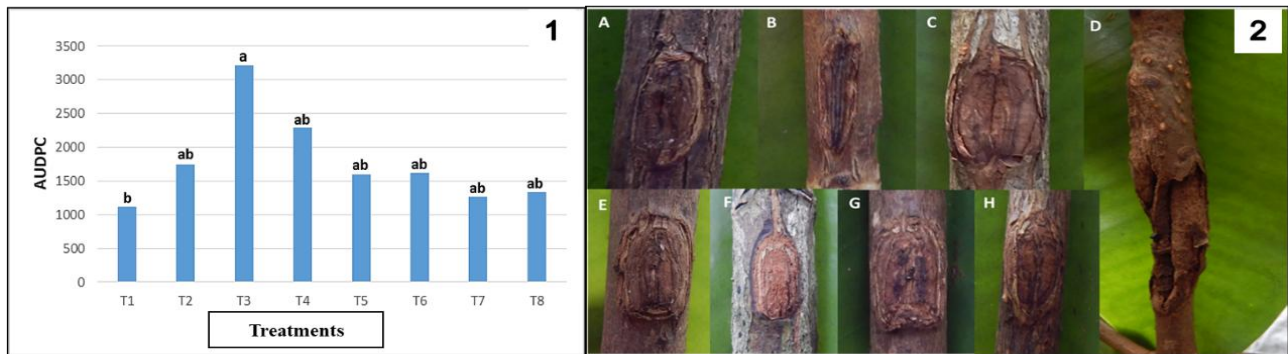


Fig. 17 – (1) Bar graphic showing pathogenicity test results under field conditions. Bars represent AUDPC average values of seven replicates; different letters in the columns mean statistical differences between treatments using Tukey’s test ($P < 0.01$). **(2)** Lesions on *R. mangle* caused by inoculations of fungi under field conditions after 30 weeks. A. Control agar disc. B. Control water. C. Morphotype 1 agar disc. D. Morphotype 1 conidial suspension. E. Morphotype 2 agar disc. F. Morphotype 6 agar disc. G. Morphotype 17 agar disc. H. Morphotype 21 agar disc.

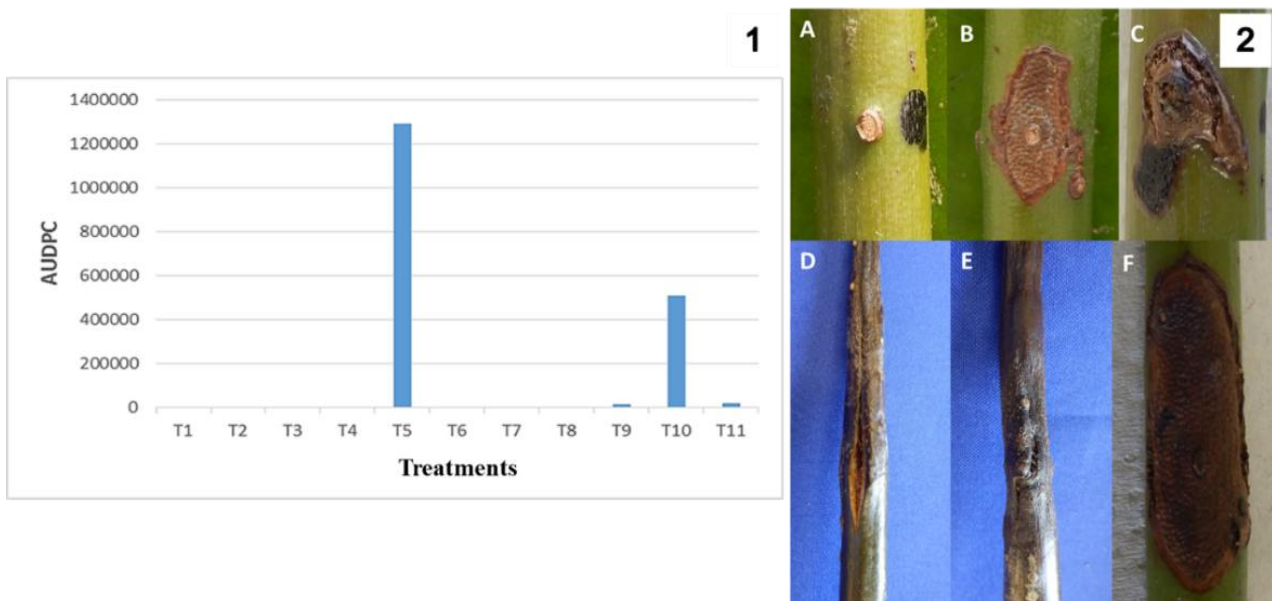


Fig. 18 – (1) Bar graphic showing pathogenicity test results under greenhouse conditions. Bars represent the averaged AUDPC values of seven replicates; different letters in the columns mean statistical differences between treatments using Tukey’s test ($P < 0.01$). **(2)** Lesions on *R. mangle* caused by inoculations of fungi under greenhouse conditions after 176 days. A. Control. B. *R. rugulosa*. C. Morphotype 1. D. *L. jatrophiicola* plus morphotype 1. E, F. *L. jatrophiicola*.

Discussion

The incidence of gall disease among the *Rhizophora mangle* trees in the surveyed plots was moderate to high (Mira-Martinez et al. 2017). Most trees had galls along the stem and prop roots, whereas older trees showed cankers and galls. Conidial orange cirrus was observed exuding from cankers and galls more frequently during the high rainy season. A complex of fungi species was implicated in the development of this disease, including an unidentified species of the Cryphonectriaceae, two species of *Lasiodiplodia* (*L. jatrophiicola* and *L. theobromae*), *Cytospora*

rhizophorae and *Rugonectria rugulosa*. Inoculation tests showed that only the unidentified Cryphonectriaceae and *Lasiodiplodia* species were pathogenic on *Rhizophora mangle* individuals, inducing disease symptoms on inoculated stems under field and greenhouse conditions. *C. rhizophorae* and *R. rugulosa* were weak pathogens.

Isolates of the Cryphonectriaceae (Mph 1) and *Lasiodiplodia* species showed the highest prevalence on *R. mangle* in trees of the evaluated plots. Unidentified Cryphonectriaceae was present in 10 of 13 plots, and *Lasiodiplodia* species was evaluated in 11 of the 13 plots. These fungi were consistently isolated from the stems and prop root tissues of *Rhizophora mangle*, that showed gall and canker disease symptoms.

Cryphonectriaceae species can be virulent plant pathogens, facultative parasites or saprobes. They live within the bark and wood of trees and have a worldwide distribution and include some of the world's most important pathogens of trees, that cause such as canker disease of eucalyptus (*Chrysosporthe cubense*) and chestnut blight (*Cryphonectria parasitica*) (Gryzenhout et al. 2009).

Genera within the Cryphonectriaceae differ from other families or groups in the Diaporthales order by the presence, both in culture and in host, of orange stromatal tissue (Gryzenhout et al. 2009). Most anamorphs of Cryphonectriaceae have orange or yellow conidiomata and / or ascomata, unlike *Aurapex*, *Celoportha*, *Chrysosporthe* and *Luteocirrhus*, which present dark brown to black pycnidia, a characteristic that resembles that observed in isolates of the unidentified Cryphonectriaceae (Mph 1). These red mangrove tissue isolates showed a higher morphological affinity with *Luteocirrhus*, both exhibiting brown to black conidiomata, pulvinate to globose, without necks (short and attenuated in *Luteocirrhus*), superficial to semi-immersed, erumpent (superficial for *Luteocirrhus*; immersed for Mph 1), ostiolate, uni- to multilocular. Conidiophores were hyaline and filamentous, and conidia were hyaline, aseptate, straight or slightly allantoid, exuding as orange cirrus or yellow droplets. Sexual structures were absent in both genera.

Comparisons of DNA sequence data from the TUB2, ITS and LSU gene regions have been used in biological diversity and multilocus phylogeny studies of the Cryphonectriaceae (Gryzenhout et al. 2009). Nuclear genes that encode proteins such as β -tubulin 1 and 2, EF1- α , ACT and Calmodulin (CAL), potentially are character-rich regions for speciation studies (Beier et al. 2015). In this study, sequence data from the ITS and TUB2 regions were used in combination with morphological characteristics of the asexual morphs to describe an unknown genus and species in the Cryphonectriaceae, pathogenic to *Rhizophora mangle* trees in the Urabá Gulf at the northwestern Caribbean coast of Colombia. However, further phylogenetic and evolutionary analyses will be required to clarify the taxonomic placement of these Mph 1 isolates belonging to this family. The present study provides sequences of the EF1- α and ACT partial genes for Mph 1, which may support future taxonomic analysis of this group. To our knowledge, this is the first report of a fungus in the *Cryphonectriaceae* as a pathogen on red mangrove.

Species of *Lasiodiplodia* are common fungi in tropical and subtropical areas and have a wide range of hosts (both monocotyledonous and dicotyledonous angiosperms, and gymnosperms). Generally, they exhibit diverse lifestyles including endophytes, pathogens that cause disease in various plant hosts and saprobes commonly found on dead woody plant tissues (Slippers & Wingfield 2007, Alves et al. 2008, De Silva et al. 2019).

Lasiodiplodia is a genus of the Botryosphaeriaceae (Botryosphaeriales, Dothideomycetes, Ascomycota). This family is characterized by large, ovoid to oblong, usually hyaline, aseptate ascospores and hyaline or pigmented, aseptate, one or rarely multi-septate, thick-walled conidia, usually with longitudinal striations. *Lasiodiplodia* species differ from other closely related genera in the Botryosphaeriaceae by the presence of pycnidial paraphyses and longitudinal striations on mature conidia. Morphology of conidia and paraphyses are used for species delimitation (De Silva et al. 2019).

Morphologically species of the Botryosphaeriaceae are characterized by fast growing colonies on PDA, with growth rates of 6–25 mm/day (Crous et al. 2006), a range in which Mph 3 isolates were found. Species in genus *Lasiodiplodia* usually have whitish mycelium when young then turn

grayish brown with age and aerial mycelium being coarse in texture (Abdollahzadeh et al. 2010), as was observed in isolates of Mph 3. However, according to Phillips et al. (2013) macroscopic morphological characters are not decisive in the classification of genera within the Botryosphaeriaceae.

Microscopically, conidia of the *Lasiodiplodia*-like genera have unicellular or 1-septate cells, with relatively thick, smooth walls, hyaline or brown. In *Lasiodiplodia*, conidia generally remain hyaline long after they form but can turn brown with 1-septum with age. However, pigmentation and septation normally occur after discharged. In some species, assigned to the genera *Lasiodiplodia* and *Neodeightonia*, conidia take on a striated appearance due to melanin deposits that accumulate on the inner wall surfaces and are arranged in longitudinal rows (Alves et al. 2008). Accordingly, to these morphological characteristics, Mph 3 isolates could be assigned to *Lasiodiplodia* and *Neodeightonia* genera.

Abdollahzadeh et al. (2010) using a combined analysis of ITS and EF1- α sequence data separated 21 species of the genus *Lasiodiplodia*, such as *L. citricola*, *L. parva*, *L. hormozganensis*, which are mainly distinguishable by differences in their EF1- α sequences. Later Phillips et al. (2013) and Slippers et al. (2014) proposed that species can be recognized only from combined ITS and EF1- α sequence data. This genus comprises 31 species. Both sexual and asexual morphs have been reported within the genus. In this study, the identification of Mph 3 isolates to genus and species level was confirmed using an ITS and EF1- α combined sequence analysis. Eleven red mangrove isolates were identified as *L. jatrophiicola* and one as *L. theobromae*.

Based on the results of the pathogenicity tests under field conditions *Lasiodiplodia jatrophiicola* and the unidentified Cryphonectriaceae species (Mph 1) were found to be the most pathogenic on *R. mangle* young trees. Inoculations with Mph 1 isolate showed conidia to be more infective than mycelium. Red mangrove seedlings inoculated with conidia suspension developed larger canker lesions and showed higher tissue deformation. This symptom was observed in 57.14% of the inoculated *Rhizophora mangle* seedlings. On the other hand, *R. mangle* seedlings were more susceptible to *L. jatrophiicola* isolate using the agar plug inoculation method. A total of 66.66% of seedlings developed disease symptoms. Both fungi species induce the development of cankers and internal tissue necrosis; however, *L. jatrophiicola* was the most aggressive. Statistical analyses supported these findings and indicated a higher infection potential in *L. jatrophiicola* than in the unidentified Cryphonectriaceae isolate. These results are consistent with previous reports of different Botryosphaeriaceae genera (*Botryosphaeria*, *Fusicoccum*, *Lasiodiplodia*, and *Noefusicoccum*) associated with mangrove trees in the Americas and Asia (*R. mangle* and *R. mucronata*) (De Souza et al. 2013, Osorio et al. 2017).

Inoculation under greenhouse conditions showed that Cryphonectriaceae (Mph 1), *L. jatrophiicola*, and *R. rugulosa* are pathogenic on *R. mangle* trees when they are inoculated on lenticels without tissue injury. Results from dual inoculation of Cryphonectriaceae and *L. jatrophiicola* on lenticels showed a higher infection capacity of both fungi. Simultaneous inoculation of the two fungi appears to enhance the pathogenic potential reflected in the development of larger lesions, compared to those developed in plants inoculated with each fungus individually. *L. jatrophiicola* seems to favor infection by Mph 1 and allows a faster development of symptoms and higher disease severity.

The results of the pathogenicity test for *Cytospora rhizophorae* and *Rugonectria rugulosa* (anamorph *Cylindrocarpon*) showed these two fungi as weak pathogens of *Rhizophora mangle*. Our findings differ from those reported by Wier et al. (2000) regarding the pathogenicity of *Cytospora rhizophorae*, in which they indicated this fungus species as the causal agent of gall disease on *Rhizophora mangle* trees in Puerto Rico. Although some research reports indicate *Cylindrocarpon didymum* is the causative agent of galls and cancers in mangroves, these did not include studies that demonstrate the pathogenicity of this fungus or the reproduction of disease symptoms in *Rhizophora mangle* (Olexa & Freeman 1978, Bernard & Freeman 1982). These and other studies showed that *Cytospora rhizophorae* and *C. didymum* are opportunistic fungi attacking debilitated or stressed mangrove trees due to environmental conditions (Olexa & Freeman 1978, Teas 1982, Wier et al. 2000).

Studies by Wier et al. (2000) in the southwest of Puerto Rico determined that environmental changes in mangrove forests, such as high incidence of wounds and salinity may predispose mangroves to *C. rhizophorae* infection. However, studies conducted in coastal forests have shown that fungal species distribution is influenced by salinity, with a few species present under high salt concentration. Therefore, disease pressure may increase in less saline environments (Jones 2000, Gilbert et al. 2002), which may explain the high incidence of gall disease on the *Rhizophora mangle* trees on mangroves of the Atrato River delta. In this area salt concentrations are lower than in other mangroves of the Urabá Gulf. Additionally, high alluvial sedimentation rate, high percentage of soil organic matter and higher concentrations of Cu, Zn and As in the soils, are related to anthropogenic disturbances (Singh et al. 2010, Urrego et al. 2014, Betancur 2018). In addition, uncontrolled expansions of urban infrastructure and banana crops, pollutants derived from mining, and natural disturbances act as environmental stressors for *R. mangle* trees, increasing their predisposition and susceptibility to gall and canker pathogens.

In general, *Cytospora* and *Cylindrocarpon* species are considered effective wound parasites that attack weakened trees, causing cankers and eventually host death, because of their direct infections or their invasion as secondary organisms (Schoeneweiss 1975, McIntyre Jacobi & Ramaley 1996). Some of these species are considered endophytes, colonizers of asymptomatic bark and xylem tissues of woody plants; they colonize wood when water content in branches and stems decreases below a certain level (Fisher et al. 1993, Adams et al. 2005, Adams et al. 2006, González & Tello 2011). Drought stressed trees are more prone to develop canker symptoms caused by species of *Cytospora* and *Lasiodiplodia* (Guyon Jacobi & McIntyre 1996, Kepley & Jacobi 2000). High precipitation, low seasonality, and salinity may be associated with the low infection capacity of these species in trees of the study area.

Mangroves are forests subjected to constant environmental changes that affect their structural conditions, making them in many cases more susceptible to pathogenic and endophytic fungi such as *Cytospora*, *Cylindrocarpon* and *Lasiodiplodia*. Osorio et al. (2017) reported the occurrence of endophytic Botryosphaeriaceae along mangrove forest of South Africa, where they found 14 species of Botryosphaeriaceae associated with mangrove species. Species in the genera *Lasiodiplodia*, *Neofusicoccum*, *Diplodia* and *Botryosphaeria* were isolated from six South African mangrove species, not including *R. mangle* (Osorio et al. 2017). These findings indicate a rich diversity of fungi in the Botryosphaeriaceae living as endophytes in mangrove forests, with *Lasiodiplodia avicenniae* being highly pathogenic to *Avicennia marina* (Osorio et al. 2017).

In this study we found *Lasiodiplodia jatrophicola* and *L. theobromae* associated with *R. mangle*, the latter one already reported as an endophytic fungus in *Barringtonia racemosa* in Brazil. These findings constitute the first report of *L. jatrophicola* as a potential pathogen of *R. mangle* and the causal agent of canker diseases under field conditions and stem necrosis of seedlings under greenhouse conditions, and it also constitutes the fourth report of a new host for this species.

Reports of fungi in the Cryphonectriaceae affecting mangroves are scarce so far. De Souza et al. (2013) recorded *Chrysosporthe cubensis* isolated from leaf tissue of *Avicennia nitida*, and four isolates in the genus *Endothia*, three of *E. viridistroma* and one of *E. gyrosa*, isolated from the leaves of *Rhizophora mangle* and branches of *Lasiodiplodia racemosa* as endophytic fungi of mangroves. Worldwide, there is only one report of pathogenic fungi in the Cryphonectriaceae on *Rhizophora mangle*. Seixas et al. (2004) evaluated the host range of *Chrysosporthe cubensis* by artificial inoculation of 40 plant species including *Rhizophora mangle*. The plants were evaluated 30 days after inoculation using a disease severity scale of 0 to 3. Plants of *R. mangle* showed a 3-grade disease severity, leading researchers to consider *Chrysosporthe cubensis* as a pathogen able to infect a wide range of hosts throughout the tropics, including mangrove species.

Although most studies in the Cryphonectriaceae fungi have focused on *Eucalyptus* species due to their economic importance, it is imperative to study these fungi in other geographic areas and host, because they could be potential pathogens to other plant species different from their original host (Seixas et al. 2004, Crous et al. 2006).

The accidental movement of fungi into new environments and the epidemics of diseases that have arisen subsequently generate growing concern because, in some cases, the incidence and impact of these introductions have increased (Desprez et al. 2006). Live plant trade, sometimes called "seed plants," and wood (asymptomatic) have been identified as two main pathways for pathogen introduction into new regions.

This suggests that some fungi in the Cryphonectriaceae may exist probably exist as endophytes in different hosts. These may explain many of the recent and surprising canker outbreaks caused by Cryphonectriaceae species, particularly in South America, South Africa, and Southwest Asia (Myburg et al. 2003, Gryzenhout et al. 2004, Roux & Apetorgbor 2010).

Globally, emerging diseases caused by foreign fungi are constantly increasing. Climate change is seen as the driving force behind the emerging pathogenicity of normally minor pathogens (Desprez et al. 2006, Dakin et al. 2010). For example, low temperature contributes to magnified disease cankers in plants of the Proteaceae caused by a complex of fungi, including *Neofusicoccum australe*, *N. macroclavatum*, *Cryptodiaporthe melanocraspeda*, and *Luteocirrhus sharia* (Crane & Burgess 2013).

In summary, this research aligns with the scientific community's calls for more research on fungal biodiversity in the American continent, especially those associated with fungi in non-commercial tropical forests. The results obtained in the present study are expected to strengthen knowledge about pathogens and "new encounter" diseases, both of economic and ecological importance worldwide.

Acknowledgements

This work was funded by grant No.4600001029 from the Government of Antioquia, Secretary of Environment. We thank Universidad Nacional de Colombia for partial financial support, Guillermo A. Correa for data analysis assistance, and Bocas del Atrato community for their support during field sampling.

Disclosure statement

The authors declare no conflict of interest.

Supplementary Material

Supplementary materials are presented in: Table S1.

References

- Abdollahzadeh J, Javadi A, Mohammadi Goltapeh E, Zare R et al. 2010 – Phylogeny and morphology of four new species of *Lasiodiplodia* from Iran. *Persoonia: Molecular Phylogeny and Evolution of Fungi*, 25, 1–10. Doi 10.3767/003158510X524150.
- Adams GC, Roux J, Wingfield MJ. 2006 – *Cytospora* species (Ascomycota, Diaporthales, Valsaceae): Introduced and native pathogens of trees in South Africa. *Australasian Plant Pathology*, 35(5): 521–48.
- Adams GC, Wingfield MJ, Common R, Roux J. 2005 – Phylogenetic relationships and morphology of *Cytospora* species and related teleomorphs (Ascomycota, Diaporthales, Valsaceae) from eucalyptus - Preface. *Studies in Mycology*, (52): 1–144.
- Afanador-Kafuri L, González A, Gañán L, Mejía JF et al. 2014 – Characterization of the *Colletotrichum* species causing anthracnose in Andean blackberry in Colombia. *Plant Disease*, 98: Doi 10.1094/PDIS-07-13-0752-RE
- Alves A, Crous PW, Correia A, Phillips AJL. 2008 – Morphological and molecular data reveal cryptic speciation in *Lasiodiplodia theobromae*. *Fungal Diversity*, 28: 1–13.
- Badullage1 HS, Mallawaarachchi TT, Jayapala HPS, Chaturani SHU et al. 2023. Diseases and Pathogens Associated with Mangrove Ecosystems; A Systematic Review. *Proceedings of the International Conference on Mangroves for Ecological & Economic Sustainability*. July 26

- Barnett HL, Hunter BB. 2006 – Illustrated genera of imperfect fungi. 4^a ed. (T.A.P. Society, Ed.). The American Phytopathological Society, St. Paul, MN, USA.
- Beier GL, Hokanson S C, Bates ST, Blanchette RA 2015 – *Aurantioporthe corni* gen. et comb, nov., an endophyte and pathogen of *Cornus alternifolia*. Mycologia, 107: Doi 10.3852/14-004
- Bernard E, Freeman E. 1982 – *Cylindrocarpon* galls on red mangrove. Plant Pathology, 2p. (Circular, 235).
- Betancur Valencia S. 2018 – Galls on *Rhizophora mangle* L.: relationship with environmental variables and effects on vegetation. Master Thesis. Universidad Nacional de Colombia, Medellín, Colombia. 48p.
- Blanco JF, Taborda A, Amortegui V, Arroyave A et al. 2013 – Deforestación y sedimentación en los manglares del Golfo de Urabá síntesis de los impactos sobre la fauna macrobéntica e íctica en el delta del río Turbo. Gestión y Ambiente, 16(2): 19–36.
- Carbone I, Anderson JB, Kohn LM. 1999 – Patterns of descent in clonal lineages and their multilocus fingerprints are resolved with combined gene genealogies. Evolution 53(1): 11–21.
- Carbone I & Kohn LM (1999) Carbone, I., & Kohn, L. M. 1999. A method for designing primer sets for speciation studies in filamentous ascomycetes. Mycologia, 91(3), 553–556.
- Chaverri P, Salgado C, Hirooka Y, Rossman AY, Samuels GJ. 2011. Delimitation of *Neonectria* and *Cylindrocarpon* (Nectriaceae, Hypocreales, Ascomycota) and related genera with *Cylindrocarpon*-like anamorphs, Studies in Mycology, Volume 68, Pages 57-78.
- Correa ID, Vernet G. 2004 – Introducción al problema de la erosión litoral de Urabá (sector Arboletes-Turbo) costa Caribe colombiana. Boletín de Investigaciones Costeras y Marinas, 33: 7–28.
- Crane C, Burgess TI. 2013 – *Luteocirrhus shearii* gen. sp. nov. (Diaporthales, Cryphonectriaceae) pathogenic to Proteaceae in the Southwestern Australian Floristic Region. IMA Fungus 4: Doi 10.5598/ima fungus.2013.04.01.11ertype= abstract.
- Crous PW, Slippers B, Wingfield MJ, Rheeder J et al. 2006 – Phylogenetic lineages in the Botryosphaeriaceae. *Studies in Mycology*, 55, 235–253. Retrieved from <http://ncbi.nlm.nih.gov/pmc/articles/PMC2104729>
- Dakin N, White D, Hardy GESJ, Burgess TI. 2010 – The opportunistic pathogen, *Neofusicoccum australe*, is responsible for crown dieback of peppermint (*Agonis flexuosa*) in Western Australia. Australasian Plant Pathology, 39(2): 202–206. Doi 10.1071/AP09085
- De Silva NI, Phillips AJ, Liu JK, Lumyong S et al. 2019 – Phylogeny and morphology of *Lasiodiplodia* species associated with *Magnolia* Forest plants. Scientific reports, 9(1), 14355.
- De Souza Sebastianes FL, Romão–Dumaresq AS, Lacava PT, Harakava R et al. 2013 – Species diversity of culturable endophytic fungi from Brazilian mangrove forests. Current Genetics, 59(3): 153–166. Doi 10.1007/s00294-013-0396-8
- Desprez–Loustau ML, Marçais B, Nageleisen LM, Piou D et al. 2006 – Interactive effects of drought and pathogens in forest trees. Ann. For. Sci., 63(6): 597–612. Doi 10.1051/forest:2006040
- Drummond AJ, Suchard MA, Xie D, Rambaut A. 2012 – Bayesian Phylogenetics with BEAUti and the BEAST 1.7. Molecular Biology and Evolution, 29(8), 1969–1973. Retrieved from Doi 10.1093/molbev/mss075
- Duke NC, Meynecke JO, Dittmann S, Ellison AM et al. 2007 – A world without mangroves? Science, 317(5834): 41b–42b. Doi 10.1126/science.317.5834.41b
- Edgar RC. 2004 – MUSCLE: multiple sequence alignment with high accuracy and high throughput. Nucleic Acids Research, 32(5):1792-1797.
- Fisher PJ, Petrini O, Sutton BC. 1993 – A comparative study of fungal endophytes in leaves, xylem and bark of *Eucalyptus* in Australia and England. Sydowia, 45(2): 338–345. Doi 10.1016/S0953-7562(09)80356-0
- Gilbert GS, Mejía–Chang M, Rojas E. 2002 – Fungal diversity and plant disease in mangrove forests: salt excretion as a possible defense mechanism. Oecología 132: 278–285. Doi 10.1007/s00442-002-0966-9

- Gilman E, Ellison J, Duke N, Field CN. 2008 – Threats to mangroves from climate change and adaptation options. *Aquatic Botany*, 89: 237–250.
- Glass NL, Donaldson GC. 1995 – Development of primer sets designed for use with the PCR to amplify conserved genes from filamentous ascomycetes. *Appl Environ Microbiol* 61(4):1323–30. Doi 10.1128/aem.61.4.1323–1330.1995. PMID: 7747954; PMCID: PMC167388.
- González V, Tello ML 2011 – The endophytic mycota associated with *Vitis vinifera* in central Spain. *Fungal Diversity*, 47(1): 29–42. Doi 10.1007/s13225–010–0073–x
- Goudarzi A, Moslehi M. 2020- Distribution of a devastating fungal pathogen in mangrove forests of southern Iran. *Crop Protection* 128. 104987
- Gryzenhout M, Myburg H, Van Der Merwe NA, Wingfield BD et al. 2004 – *Chrysosporthe*, a new genus to accommodate *Cryphonectria cubensis*. *Studies in Mycology* 50:119–142.
- Gryzenhout M, Tarigan M, Clegg PA, Wingfield MJ. 2009 – Taxonomy, phylogeny, and ecology of bark-infecting and tree killing fungi in the *Cryphonectriaceae*. *Aust Plant Pathol* 39: 161–69.
- Guyon JC, Jacobi WR, McIntyre GA. 1996 – Effects of environmental stress on the development of *Cytospora* canker of aspen pdf. *Plant Disease*, 80(12): 1320–1323. https://digitalcommons.usu.edu/aspen_bib/1765
- Hasegawa M, Kishino H, Yano T. 1985 – Dating of the human–ape splitting by a molecular clock of mitochondrial DNA. *J Mol Evol*. 22:160–174.
- Hoyos R, Urrego LE, Lema A. 2012 – Respuesta de la regeneración natural en manglares del golfo de Urabá (Colombia) a la variabilidad ambiental y climática intra–anual. *Revista de Biología Tropical*, 61 (3): 1445–1461.
- Jones E. 2000 – Marine fungi: some factors influencing biodiversity. *Fungal Diversity*, 4: 53–73.
- Kepley JB, Jacobi WR. 2000 – Pathogenicity of *Cytospora* fungi on six hardwood species. *Journal of Arboriculture*, 26(6): 326–333. Available at: <https://scopus.com/inward/record.uri?eid=2–s2.0–0034495129&partnerID=40&md5=1370c64d5db522d7450b6e043976ad8c>
- Kimura M. 1980 – A simple method for estimating evolutionary rate of base substitutions through comparative studies of nucleotide sequences. *Journal of Molecular Evolution* 16:111–120.
- Krauss KW, Lovelock CE, McKee KL, López–Hoffman L et al. 2008 – Environmental drivers in mangrove establishment and early development: A review. *Aquatic Botany*, 89(2), 105–127. Doi 10.1016/j.aquabot.2007.12.014
- Krauss KW, McKee KL, Lovelock CE, Cahoon DR et al. 2014 – How mangrove forests adjust to rising sea level. *New Phytologist*, 202: 19–34 Doi 10.1111/nph.12605
- Kumar S, Stecher G, Li M, Knyaz C et al. 2018 – MEGA X: molecular evolutionary genetics analysis across computing platforms. *Molecular Biology and Evolution*, 35(6): 1547–1549.
- Lombard, Lorenzo & van der Merwe, Nicolaas & Groenewald, E. & Crous, Pedro. (2014). Lineages in Nectriaceae: Generic status of *Fusarium*. *Studies in Mycology* 80: 189–245.
- Lombard L, Van der Merwe NA, Groenewald JZ, Crous PW. 2015 – Generic concepts in Nectriaceae. *Studies in Mycology* 80, 189–245.
- Lugo A.E, S.C. Snedaker. 1974 – The ecology of mangroves. *Annual Review of Ecology and Systematics* 5: 39–64.
- McIntyre GA, Jacobi WR, Ramaley AW. 1996 – Factors affecting *Cytospora* canker occurrence on aspen. *Journal of Arboriculture*, 22: 229–233.
- McKee KL, Cahoon DR, Feller IC. 2007 – Caribbean mangroves adjust to rising sea level through biotic controls on change in soil elevation. *Global Ecology and Biogeography* 16: 545–556.
- Mira–Martínez JD, Betancur–Valencia S, Urrego–Giraldo LE. 2017 – Relación entre la infección por agallas, las variables estructurales y la anatomía de la madera de *Rhizophora mangle* L., en el golfo de Urabá (Colombia). *Actualidades Biológicas* 39(106): 41–52
- Munsell Soil Color Charts. 1990 – Edition Revised. Munsell Color, Macbeth Division of Kollmorgen Instruments Corporation, 2441 North Calvert Street, Baltimore, Maryland, 21218.
- Myburg H, Gryzenhout M, Wingfield BD, Wingfield MJ. 2003 – Conspecificity of *Endothia eugeniae* and *Cryphonectria cubensis*: A re-evaluation based on morphology and DNA sequence data. *Mycoscience*, 44(3): 187–196. Doi: 10.1007/S10267–003–0101–8

- Norphanphoun C, Raspé O, Jeewon R, Wen T-C et al. 2018 – Morphological and phylogenetic characterisation of novel *Cytospora* species associated with mangroves. *MycKeys* 38: 93–120. 28011
- Olexa MT, Freeman TE. 1978 – A gall disease of red mangrove caused by *Cylindrocarpon didymium*. *Plant Disease Reporter*, 62: 283–286.
- Osorio JA, Crous CJ, de Beer ZW, Wingfield MJ et al. 2017 – Endophytic Botryosphaeriaceae, including five new species, associated with mangrove trees in South Africa. *Fungal Biology*, 121(4): 361–393. Doi 10.1016/j.funbio.2016.09.004
- Phillips AJL, Alves A, Abdollahzadeh J, Slippers B et al. 2013 – The Botryosphaeriaceae: Genera and species known from culture. *Studies in Mycology*, 76: 51–167. Doi: 10.3114/sim0021
- Ronquist F, Huelsenbeck JP. 2003 – MrBayes 3: Bayesian phylogenetic inference under mixed models. *Bioinformatics*, 19: 1572–1574.
- Roux J, Apetorgbor M. 2010 – First report of *Chrysosporthe cubensis* from Eucalyptus in Ghana. *Plant Pathology*, 59(4): 806. Doi 10.1111/j.1365-3059.2009.02252.x
- Sánchez-Alfárez A, Álvarez-León R, Godoy Bueno S, Lopez C et al. 2009 – Caribe Colombiano, 4(26): 339–346.
- Schoeneweiss DF. 1975 – Predisposition, stress, and plant disease. *Annual Review of Phytopathology*, 13(1): 193–211. Doi 10.1146/annurev.py.13.090175.001205
- Seixas CDS, Barreto RW, Alfenas AC, Ferreira FA. 2004 – *Cryphonectria cubensis* on an indigenous host in Brazil: a possible origin for eucalyptus canker disease? *Mycologist*, 18(1): 39–45. Doi: 10.1017/S0269915X04001077
- Singh G, Ranjan RK, Chauhan R, Ramanathan AL. 2010 – Dissolved metal distribution in Indian mangrove ecosystem: case studies from East Coast of India. In: Ramanathan, et al. (Eds.), *Management and Sustainable Development of Coastal Zone Environments*. Springer, Germany, ISBN 978-90-481-3067-2.
- Slippers B, Wingfield MJ. 2007 – Botryosphaeriaceae as endophytes and latent pathogens of woody plants: diversity, ecology and impact. *Fungal Biology Reviews*, 21(2–3): 90–106. Doi 10.1016/j.fbr.2007.06.002
- Slippers B, Roux J, Wingfield MJ, van der Walt FJ et al. 2014 – Confronting the constraints of morphological taxonomy in the Botryosphaeriales. *Persoonia* 33:155–68.
- Suárez JA, Urrego LE, Osorio A, Ruiz HY. 2015 – Oceanic and climatic drivers of mangrove changes in the Gulf of Urabá, Colombian Caribbean. *Latinoamerican Journal of Aquatic Research*, 43(5): 972–985 Doi 10.3856/vol43-issue5-fulltext-17.
- Teas HJ. 1982 – An epidemic dieback gall disease of *Rhizophora* mangroves in the Gambia, West Africa. *Plant Disease*, 66(6): 522–523.
- Urrego LE, Molina EC, Suárez JA, Ruiz HY et al. 2010 – Distribución, composición y estructura de los manglares del golfo de Urabá. Expedición Estuarina, Golfo de Urabá, Fase 1. Expedición Caribe Sur Antioquia y Chocó Costeros, 22.
- Urrego LE, Molina EC, Suárez JA. 2014 – Environmental and anthropogenic influences on the distribution, structure, and floristic composition of mangrove forests of the Gulf of Urabá (Colombian Caribbean). *Aquatic Botany*, 114: 42–49.
- Weising K, Nybom H, Pfenninger M, Wolff K et al. 1994 – DNA fingerprinting in plants and fungi. CRC press.
- White T, Bruns T, Lee S, Taylor J. 1990 – Amplification and Direct Sequencing of Fungal Ribosomal RNA Genes for Phylogenetics. In: PCR Protocols: A Guide to Methods and Applications. Eds. N. Innis D. Gelfand, J. Smith, and T. White. Academic Press, New York. pp. 315–322.
- Wier AM, Tattar T. 2000 – Disease of Red Mangrove (*Rhizophora mangle*) in southwest Puerto Rico caused by *Cytospora rhizophorae*. *Biotropica*, 32(2): 299–306.

SUPPLEMENTARY TABLE 1

Table S1 GeneBank accession numbers of fungi isolates from *Rhizophora mangle* and related GeneBank accessions of taxa include in this study.

Fungi species	Isolate code	GenBank accession numbers ¹		
		ITS	TUB 2	EF1- α
<i>Latruncellus aurorae</i>	CMW 28274	GU726946.1	GU726958.1	-
<i>Latruncellus aurorae</i>	CMW 28275	HQ171209.1	HQ171207.1	-
<i>Immersiporthe knoxdaviesiana</i>	CMW 37314	JQ862765.1	JQ862775.1	-
<i>Immersiporthe knoxdaviesiana</i>	CMW 37315	JQ862766.1	JQ862786.1	-
<i>Microthia havanensis</i>	CMW 14550	DQ368735.1	AH015792.2	-
<i>Microthia havanensis</i>	CMW 11298	AY214320.1	AY214248.1	-
<i>Ursicollum fallax</i>	CMW 18115	DQ368756.1	AH015659.2	-
<i>Ursicollum fallax</i>	CMW 18119	DQ368755.1	AH015658.2	-
<i>Aurapex penicillata</i>	CMW 10030	AY214311.1	AY214239.1	-
<i>Aurapex penicillata</i>	CMW 10035	AY214313.1	AY214241.1	-
<i>Holocryphia eucalypti</i>	CMW 7036	AY194105.1	AH011603.2	-
<i>Holocryphia eucalypti</i>	CMW 37257	KF156758.1	KF309270.1	-
<i>Celoporthe eucalypti</i>	CMW 26900	HQ730836.1	HQ730816.1	-
<i>Celoporthe eucalypti</i>	CMW 12750	HQ730830.1	HQ730810.1	-
<i>Cryptometrion aestuescens</i>	CMW 18793	MH863328.1	GQ369456.1	-
<i>Cryptometrion aestuescens</i>	CMW 18790	GQ369458.1	GQ369455.1	-
<i>Cryphonectria nitschkei isolate</i>	CMW 13742	AY697936.1	AH014588.2	-
<i>Cryphonectria macrospora</i>	YMJ 94031513	EF026116.1	EF025618.1	-
<i>Cryphonectria parasitica</i>	CMW 13749	JN942326.1	AH014579.2	-
<i>Aurantioporthe corni</i>	MNS1002	KF495042.1	KF495072.1	-
<i>Aurantioporthe corni</i>	IAS1001	KF495037.1	KF495067.1	-
<i>Luteocirrhus shearii</i>	CBS 130774	KC197020.1	KC197011.1	-
<i>Luteocirrhus shearii</i>	CBS 130775	KC197024.1	KC197015.1	-
<i>Endothia gyrosa</i>	CMW 2091	AF046905.2	AH011601.2	-
<i>Endothia gyrosa</i>	CRY1522/E27	AF368326.1	AH011602.2	-
<i>Chrysoporthe hodgesiana</i>	CMW 10625	JN942328.1	AH014900.2	-
<i>Chrysoporthe inopina</i>	CMW 12729	DQ368778.1	AH015656.2	-
<i>Chrysoporthe cubensis</i>	CMW 11290	AY214304.1	AY214232.1	-
<i>Rostraureum tropicale</i>	CMW9971	AY167435.1	AY167425.1	-
<i>Rostraureum tropicale</i>	CMW10796	AY167438.1	AY167428.1	-
<i>Diaporthe ambigua</i>	CMW 5288	AF543817.1	AF543821.1	-
<i>Diaporthe ambigua</i>	CMW 5287	AF543818.1	AF543820.1	-
Morphotype 1	1_1	ON873716	ON887212	-
Morphotype 1	1_2	ON873717	ON887213	-
Morphotype 1	1_3	ON873718	ON887214	-
Morphotype 1	1_4	ON873719	ON887215	-
Morphotype 1	1_5	ON873720	ON887216	-
Morphotype 1	1_6	ON873724	ON887220	-
Morphotype 1	1_7	ON873721	ON887217	-
Morphotype 1	1_8	ON873725	ON887221	-
Morphotype 1	1_9	ON873722	ON887218	-

Table S1 Continued

Fungi species	Isolate code	GenBank accession numbers ¹		
		ITS	TUB 2	EF1- α
Morphotype 1	1_10	ON873723	ON887219	-
<i>Cosmospora arxii</i>	CBS 748.69	KM231819.1	-	-
<i>Cosmospora butyri</i>	DUCC4011	KP334112.1	-	-
<i>Cosmospora butyri</i>	INBio:31C	KU204560.1	-	-
<i>Cosmospora vilior</i>	E9823C	JN541223.1	-	-
<i>Cosmospora stegonsporii</i>	A.R._4385	KC291718.1	-	-
<i>Cosmospora stegonsporii</i>	UASWS1262	KP114076.1	-	-
<i>Cosmospora viridescens</i>	CBS 102430	KJ676147.1	-	-
<i>Cosmospora cymosa</i>	CBS 762.69	NR_111605.1	-	-
<i>Cosmospora viridescens</i>	IMI_73377a	KJ676171.1	-	-
<i>Cylindrocarpon cylindroides</i>	CBS 324.61	JF735312.1	-	-
<i>Cylindrocarpon cylindroides</i>	CBS 503.67	AY677261.1	-	-
<i>Cylindrocarpon liriodendri</i>	-	NR_119565.1	-	-
<i>Fusarium acaciae-mearnsii</i>	NRRL34207	DQ459854.1	-	-
<i>Fusarium acaciae-mearnsii</i>	NRRL34461	DQ459853.1	-	-
<i>Fusarium acutatum</i>	CBS 138972	KT716198.1	-	-
<i>Fusarium acutatum</i>	MRC7544	KR909445.1	-	-
<i>Fusarium austroamericanum</i>	NRRL28585	DQ459839.1	-	-
<i>Fusarium austroamericanum</i>	NRRL28718	DQ459838.1	-	-
<i>Fusarium brasiliicum</i>	NRRL_31238	DQ459860.1	-	-
<i>Fusarium brasiliicum</i>	NRRL31281	DQ459861.1	-	-
<i>Fusarium cerealis</i>	S344	KP264663.1	-	-
<i>Fusarium cerealis</i>	Z308	KP264658.1	-	-
<i>Fusarium decemcellulare</i>	48.IV_18S	GU797410.2	-	-
<i>Fusarium decemcellulare</i>	C218	KU377469.1	-	-
<i>Fusarium proliferatum</i>	WLM114	KU556138.1	-	-
<i>Fusarium acaciae-mearnsii</i>	NRRL_26754	NR_121204.1	-	-
<i>Fusarium kyushuense</i>	NRRL6491	FSU85546	-	-
<i>Fusarium_kyushuense</i>	NRRL25348	FSU85547	-	-
<i>Fusarium proliferatum</i>	JINF001	KX196810.1	-	-
<i>Pseudocosmospora eutypellae</i>	A.R._4527	KC291720.1	-	-
<i>Pseudocosmospora eutypellae</i>	A.R._4562	KC291721.1	-	-
<i>Pseudocosmospora metajoca</i>	A.R._4576	KC291745.1	-	-
<i>Pseudocosmospora rogersonii</i>	G.J.S._10-297	KC291728.1	-	-
<i>Xenoacremonium falcatus</i>	CBS 400.85	KM231832.1	-	-
<i>Xenoacremonium recifei</i>	CBS	KM231834.1	-	-
	541.89_18S			
<i>Xenoacremonium recifei</i>	CBS 137.35	KM231833.1	-	-
Morphotype 2	2_6	ON875957	-	-
Morphotype 2	2_1	ON875951	-	-
Morphotype 2	2_2	ON875952	-	-
Morphotype 2	2_3	ON875953	-	-
Morphotype 2	2_5	ON875954	-	-

Table S1 Continued

Fungi species	Isolate code	GenBank accession numbers ¹		
		ITS	TUB 2	EF1- α
Morphotype 2	2_8	ON875955	-	-
Morphotype 2	2_11	ON875956	-	-
Morphotype 2	2_4	ON875958	-	-
Morphotype 2	2_14	ON875959	-	-
<i>Lasiodiplodia citricola</i>	7E79	KC357299.1	KC357305.1	-
<i>Lasiodiplodia citricola</i>	7E78	KC357298.1	KC357304.1	-
<i>Lasiodiplodia theobromae</i>	L1	MT372632.1	KR260820.1	-
<i>Lasiodiplodia theobromae</i>	CRI-LP3	KU870367.1	KU870371.1	-
<i>Lasiodiplodia theobromae</i>	HD1332	KU712502.1	KU712504.1	-
<i>Lasiodiplodia pseudotheobromae</i>	CERC2313	KR261713.1	KR261737.1	-
<i>Lasiodiplodia pseudotheobromae</i>	CERC2038	KP822977.1	KP823010.1	-
<i>Lasiodiplodia gilanensis</i>	2B89	KF955689.1	KF955887.1	-
<i>Lasiodiplodia gilanensis</i>	3K59	KF955690.1	KF955888.1	-
<i>Lasiodiplodia hormozganensis</i>	CERC2043	KP822968.1	KP823004.1	-
<i>Lasiodiplodia hormozganensis</i>	CERC2045	KP822969.1	KP823005.1	-
<i>Lasiodiplodia jatrophicola</i>	CMM3610	KF234544.1	KF254927.1	-
<i>Lasiodiplodia jatrophicola</i>	DSYWK03	KJ885546.1	KJ885547.1	-
<i>Lasiodiplodia jatrophicola</i>	DSYWK05	KP297435.1	KP297436.1	-
<i>Lasiodiplodia iranensis</i>	CERC2026	KP822970.1	KP823006.1	-
<i>Lasiodiplodia iranensis</i>	CERC2029	KP822972.1	KP823007.1	-
<i>Spencermartinsia viticola</i>	CBS 117009	KF766228.1	EU673104.1	-
<i>Spencermartinsia viticola</i>	CBS 117006	AY905555.1	EU673103.1	-
Morphotype 3	3_1	ON876059	ON887223	-
Morphotype 3	3_2	ON876060	ON887224	-
Morphotype 3	3_3	ON876061	ON887225	-
Morphotype 3	3_4	ON876062	ON887226	-
Morphotype 3	3_5	ON876066	ON887230	-
Morphotype 3	3_6	ON876058	ON887222	-
Morphotype 3	3_7	ON876067	ON887231	-
Morphotype 3	3_8	ON876068	ON887232	-
Morphotype 3	3_9	ON876069	ON887233	-
Morphotype 3	3_10	ON876063	ON887227	-
Morphotype 3	3_11	ON876064	ON887228	-
Morphotype 3	3_12	ON876065	ON887229	-
<i>Clonostachys byssicola</i>	CML 2311	KC806270.1	-	-
<i>Clonostachys candelabrum</i>	F12P00GC	KT759671.1	-	-
<i>Clonostachys pseudochroleuca</i>	CML 1983	KC806264.1	-	-
<i>Clonostachys rhizophaga</i>	CML 1984	KC806274.1	-	-
<i>Clonostachys rogersoniana</i>	B133 18S	KR812215.1	-	-
<i>Clonostachys rogersoniana</i>	CBS 582.89	AF210691.1	-	-

Table S1 Continued

Fungi species	Isolate code	GenBank accession numbers ¹		
		ITS	TUB 2	EF1- α
<i>Clonostachys rosea</i>	CBS 221.72b	AF358234.1	-	-
<i>f.catenulata</i>				
<i>Geosmithia fassatae</i>	CCF4331	KF808295.1	-	-
<i>Geosmithia lavendula</i>	2277140	KF808299.1	-	-
<i>Geosmithia omnicola</i>	CNR118	KR229925.1	-	-
<i>Gliomastix masseei</i>	YIMPH30029	KP230830.1	-	-
<i>Gliomastix polychroma</i>	H98	KP184326.1	-	-
<i>Gliomastix tumulicola</i>	JCM 28371	LC133828.1	-	-
<i>Hydropisphaera fungicola</i>	AR 4170	EU344903.1	-	-
<i>Clonostachys miodochialis</i>	CBS 997.69	NR 137649.1	-	-
<i>Geosmithia microcorthyli</i>	CCF 3861 ITS	NR 137566.1	-	-
<i>Gliomastix polychroma</i>	CBS 181.27	NR 119408.1	-	-
<i>Hydropisphaera bambusicola</i>	CBS 124147	NR 119761.1	-	-
<i>Stromatonectria caraganae</i>	CBS 125579	HQ112288.1	-	-
<i>Stromatonectria caraganae</i>	CBS 127387	HQ112287.1	-	-
<i>Fusarium decemcellulare</i>	48.IV 18S	GU797410.2	-	-
<i>Fusarium decemcellulare</i>	C218	KU377469.1	-	-
<i>Ovicillium attenuatum</i>	CBS 399.86	KU382191.1	-	-
<i>Ovicillium oosporum</i>	CBS 101236	KU382203.1	-	-
<i>Heleococcum aurantiacum</i>	CBS 201.35	MH855645.1	-	-
<i>Heleococcum japonense</i>	CBS 397.67	JX158420.1	-	-
Morphotype 6	6_1	ON876176	-	-
Morphotype 6	6_2	ON876175	-	-
<i>Cytospora rhizophorae</i>	HAB16R13	HQ336045.1	-	-
<i>Cytospora rhizophorae</i>	MUCC302	EU301057.1	-	-
<i>Cytospora rhizophorae</i>	M225	KR056292.1	-	-
<i>Cytospora rhizophorae</i>	A76	KU529867.1	-	-
<i>Cytospora abyssinica</i>	CBS 116819	NR_136966.1	-	-
<i>Cytospora abyssinica</i>	CMW10181	AY347353.1	-	-
<i>Cytospora acaciae</i>	CBS_468.6	DQ243804.1	-	-
<i>Cytospora chrysosperma</i>	CFCC_89630	KF765674.1	-	-
<i>Cytospora chrysosperma</i>	CFCC_89629	KF765673.1	-	-
<i>Cytospora diatrypelloidea</i>	CMW8549	AY347368.1	-	-
<i>Cytospora diatrypelloidea</i>	M13006	KU365881.1	-	-
<i>Cytospora disciformis</i>	CMW6509	AY347374.1	-	-
<i>Cytospora disciformis</i>	CMW_6509	NR_137543.1	-	-
<i>Cytospora eucalypticola</i>	CMW40051	KF923249.1	-	-
<i>Cytospora eucalypticola</i>	CMW40052	KF923250.1	-	-
<i>Cytospora leucostoma</i>	SZ351-1	KX168600.1	-	-
<i>Cytospora leucostoma</i>	SZ351-4	KX168599.1	-	-
<i>Cytospora austromontana</i>	CMW_6735	NR_137542.1	-	-
<i>Cytospora variostromatica</i>	CBS_116858	NR_136967.1	-	-
<i>Phomopsis bougainvilleicola</i>	R-4745	JX847139.1	-	-

Table S1 Continued

Fungi species	Isolate code	GenBank accession numbers ¹		
		ITS	TUB 2	EF1- α
<i>Phomopsis bougainvilleicola</i>	SCHM_3006	AY601920.1	-	-
Morphotype 14	14_1	ON876484	-	-
Morphotype 14	14_2	ON876483	-	-
Morphotype 22	22_1	ON876485	-	-
Morphotype 22	22_2	ON876486	-	-
Morphotype 22	22_3	ON876487	-	-
<i>Nectria balsamea</i>	A.R._2798	JF832598.1	-	JF832556.1
<i>Nectria balsamea</i>	A.R._3493	JF832600.1	-	JF832559.1
<i>Nectria balsamea</i>	A.R._3495	JF832561.1	-	JF832599.1
<i>Nectria pseudotrichia</i>	CBS_551.84	HM484554.1	-	HM484532.2
<i>Nectria pseudotrichia</i>	G.J.S._09-1329	JF832647.1	-	JF832530.1
<i>Nectria pseudotrichia</i>	MAFF_241452	JF832649.1	-	JF832531.1
<i>Neonectria major</i>	6840	JF268766.1	-	JF268752.1
<i>Neonectria major</i>	CBS_240.29	JF735308.1	-	JF735782.1
<i>Neonectria major</i>	6841	JF268767.1	-	JF268753.1
<i>Rugonectria neobalansae</i>	CBS_125120	KM231750.1	-	KM231874.1
<i>Rugonectria rugulosa</i>	Y.H._10-01	JF832661.1	-	JF832545.1
<i>Rugonectria rugulosa</i>	CBS_126565	KM231749.1	-	KM231873.1
<i>Ilyonectria macrodidyma</i>	CBS_112601	JF268765.1	-	JF735833.1
<i>Ilyonectria macrodidyma</i>	CBS_112615	AY997549.1	-	JF735836.1
<i>Stromatonectria caraganae</i>	CBS_125579	MH863716.1	-	HQ112286.1
<i>Stromatonectria caraganae</i>	CBS_127387	HQ112287.1	-	HQ112285.1
Morphotype 21	21_1	ON876317	-	ON887234
Morphotype 21	21_2	ON876318	-	ON887235
Morphotype 21	21_3	ON876319	-	ON887236
Morphotype 21	21_4	ON876320	-	ON887237

¹ Abbreviations: Internal transcribed spacer (ITS), β - tubulin 2 (TUB 2) and Elongation Factor – 1(EF1)